Joint Beamforming Design and Power Splitting Optimization in IRS-Assisted SWIPT NOMA Networks

Zhendong Li, Wen Chen, *Senior Member, IEEE*, Qingqing Wu, *Member, IEEE*, Kunlun Wang, *Member, IEEE*, and Jun Li, *Senior Member, IEEE*

***Abstract*— This paper proposes a novel network framework of intelligent reflecting surface (IRS)-assisted simultaneous wireless information and power transfer (SWIPT) non-orthogonal multiple access (NOMA) networks, where IRS is used to enhance the NOMA performance and the wireless power transfer (WPT) efficiency of SWIPT. We formulate a problem of minimizing base station (BS) transmit power by jointly optimizing successive interference cancellation (SIC) decoding order, BS transmit beamforming vector, power splitting (PS) ratio and IRS phase shift while taking into account the quality-of-service (QoS) requirement and energy harvested threshold of each user. The formulated problem is non-convex optimization problem, which is difficult to solve it directly. Hence, a two-stage algorithm is proposed to solve the above-mentioned problem by applying semi-definite relaxation (SDR), Gaussian randomization and successive convex approximation (SCA). Specifically, after determining SIC decoding order by designing IRS phase shift in the first stage, we alternately optimize BS transmit beamforming vector, PS ratio, and IRS phase shift to minimize the BS transmit power. Numerical results validate the effectiveness of our proposed optimization algorithm in reducing BS transmit power compared to other baseline algorithms. Meanwhile, compared with non-IRS-assisted network, the IRS-assisted SWIPT NOMA network can decrease BS transmit power by 51.13%.**

Manuscript received November 30, 2020; revised May 14, 2021; accepted August 25, 2021. Date of publication September 8, 2021; date of current version March 10, 2022. This work was supported in part by the National Key Project under Grant 2018YFB1801102 and Grant 2020YFB1807700, in part by Shanghai Fundamental Project under Grant 20JC1416502, and in part by the NSFC under Grant 62071296. The work of Qingqing Wu was supported in part by Macau Science and Technology Development Fund under Grant 0119/2020/A3 and Grant 0108/2020/A, in part by Guangdong NSF under Grant 2021A1515011900, and in part by the Open Research Fund of National Mobile Communications Research Laboratory, Southeast University, under Grant 2021D15. The associate editor coordinating the review of this article and approving it for publication was R. Hu. *(Corresponding author: Wen Chen.)*

Zhendong Li and Wen Chen are with the Department of Electronic Engineering, Shanghai Jiao Tong University, Shanghai 200240, China (e-mail: lizhendong@sjtu.edu.cn; wenchen@sjtu.edu.cn).

Qingqing Wu is with the State Key Laboratory of Internet of Things for Smart City, University of Macau, Macau, and also with the National Mobile Communications Research Laboratory, Southeast University, Nanjing 210096, China (e-mail: qingqingwu@um.edu.mo).

Kunlun Wang is with the School of Communication and Electronic Engineering, East China Normal University, Shanghai 200241, China (e-mail: klwang@cee.ecnu.edu.cn).

Jun Li is with the School of Electronic and Optical Engineering, Nanjing University of Science Technology, Nanjing 210094, China (e-mail: jun.li@njust.edu.cn).

Color versions of one or more figures in this article are available at https://doi.org/10.1109/TWC.2021.3108901.

Digital Object Identifier 10.1109/TWC.2021.3108901

***Index Terms*— IRS, simultaneous wireless information and power transfer, non-orthogonal multiple access, IRS phase shift, power splitting ratio.**

I. Introduction

With the vigorous development of emerging services such as the Internet-of-Things (IoT) and mobile Internet, the surge in wireless devices poses unprecedented challenges to beyond fifth-generation/sixth-generation (B5G/6G) communication systems in terms of massive connectivity, spectrum efficiency, energy management, and deployment costs [1]–[3]. In order to meet the massive connectivity of future networks and the higher service requirements of users, non-orthogonal multiple access (NOMA) technology has triggered extensive discussions in academia and industry. Unlike conventional orthogonal multiple access (OMA) [4], NOMA can support multiple users to share the same resources, e.g., time, frequency, coding, etc., so it can support massive connectivity of users. Specifically, taking an instance of NOMA in the power domain, the base station (BS) uses the same resource blocks to serve multiple users, which can greatly improve the spectrum efficiency to meet the users' communication requirements [5]–[9]. For power domain NOMA transmission in the downlink, superposition coding and successive interference cancellation (SIC) techniques are applied at the BS transmitter and at the users respectively [5], [10]. As such, users with stronger channel gains can remove co-channel interference caused by users with weaker channel gains before decoding [11].

In general, existing research on NOMA considers that the users' channel conditions differ greatly, i.e., there are one type of users near the BS, and the other type of users are at the edge of the BS. In this way, the BS will allocate more transmit power to users with poor channel conditions. The main reason for this consideration is that the large difference in channel conditions will greatly release the potential of NOMA [12]. More specifically, if the difference in user channel conditions is small, the performance of NOMA is not much better than that of OMA. However, in practical scenarios, the difference in user channel conditions for the NOMA networks is not always very large. This is because the wireless channel is determined by the propagation environment, which is highly random and uncontrollable. Therefore, if the channel can be controlled and adjusted, the performance of NOMA will be greatly enhanced.

In addition, considering the requirements to provide continuous information transmission and energy transmission for large-scale low-power and energy-constrained IoT devices, simultaneous wireless information and power transfer (SWIPT) technology has attracted great attention recently. By applying SWIPT, users can obtain information and energy at the same time, which brings great convenience to the deployment of energy-constrained IoT devices [13], [14]. As one of the design schemes of practical SWIPT receivers, the power splitting (PS) scheme aims to split the signal received by the receiver into two different power streams with one part used to decode information and the other part used to harvest energy [15]. Based on the PS scheme, [16] proposed a novel integrated SWIPT receiver architecture to achieve miniaturization and energy saving of the receiver. However, for the conventional SWIPT system, the wireless power transfer (WPT) efficiency will decrease sharply as the distance increases due to severe propagation loss, which thus greatly limits the performance of the SWIPT system. If the channel conditions can be strengthened, the WPT efficiency and coverage will be improved.

Recently, intelligent reflecting surface (IRS) has been proposed as a promising cost-effective solution to control and adjust the wireless channel between transceivers [1], [17]–[19]. Furthermore, it can greatly improve the spectrum efficiency, energy efficiency, and coverage of the networks, while reducing networking costs [20], [21]. Therefore, it has received widespread attention from academia and industry [22] and has also been recognized as a key enabling for the future 6G ecosystem [23]. Specifically, IRS composed of a large number of passive reflecting elements can be easily deployed on indoor walls or buildings. It can adjust the amplitude and phase of the incident signal, and realize the reconstruction of wireless channel. Unlike conventional relays, IRS is a passive device, which only passively reflects the incident signal without signal processing, so it does not introduce additional noise [24], [25]. Unlike multiple-input multiple-output (MIMO), the required hardware cost and power consumption are much lower. These have greatly promoted the application of IRS in B5G/6G networks. Based on these significant advantages of IRS, the momentum of the IRS-assisted SWIPT NOMA networks has been stimulated. Firstly, IRS reconstructs the wireless channel to make the difference in channel conditions among users, thereby enhancing the performance of NOMA. Besides, it can improve the WPT efficiency of SWIPT system, and expand the network coverage. In short, IRS-enhanced wireless networks can meet the challenges of future B5G/6G networks in terms of massive connectivity, spectrum efficiency, energy management, and cost, etc..

The application of IRS-assisted wireless networks in different scenarios and different technologies has continued to emerge, e.g., IRS-assisted MIMO [26]–[28], IRS-assisted massive MIMO [29], IRS-assisted mobile edge computing [30], IRS-assisted unmanned aerial vehicle (UAV) communication [31], [32], IRS-assisted physical layer security [27], [28], [33]–[35] and robust beamforming design in IRS-aided MISO communications [36], etc.. In addition, many scholars are currently committed to the research of IRS-enhanced NOMA transmission [2], [37]–[42] and the research of IRS-assisted SWIPT technology [43]–[45]. For the research of IRS-enhanced NOMA, Fu *et al.* jointly optimized BS beamforming vector and IRS phase shift in the NOMA network to minimize the total transmit power [37]. In [39], Zuo *et al.* considered the NOMA network in the single-input single-output (SISO) scenario, with the goal of maximizing system throughput, jointly optimizing the decoding order, channel selection and the IRS phase shift matrix. In [2], Ni *et al.* proposed a new framework for resource allocation in multi-cell IRS-assisted NOMA networks and maximized achievable sum-rate. In [42], Zhu *et al.* proposed an IRS-assisted downlink energy-efficient multiple-input single-output (MISO) transmission scheme, which greatly reduces the transmit power by optimizing the beamforming vector and the IRS phase shifs. Meanwhile, some progress has been made in the research on IRS-assisted SWIPT. In the IRS-assisted SWIPT networks, Wu *et al.* jointly optimized the active and passive beamforming vector to increase the weighted received power of information user (IU) and energy user (EU) [43]. Meanwhile, a novel algorithm was adopted in [44] to solve the problem of maximizing the weighted received power of IU and EU under the condition of satisfying all users' QoS. Pan *et al.* optimized the weighted sum-rate in IRS-assisted MIMO SWIPT networks [45].

Although there have been many researches on IRS-assisted wireless communication networks. However, the B5G/6G network will be a more complex and changeable network. The massive connectivity, spectrum efficiency, energy management and deployment cost of the network will greatly stimulate our motivation to integrate IRS with NOMA and SWIPT in order to better satisfy the business requirements of users in IoT networks. As far as we know, the current research on IRS-assisted SWIPT NOMA networks is still in its infancy. In this paper, under the constraints of meeting the users' QoS requirements and energy harvested thresholds, we minimize the BS transmit power by jointly optimizing the SIC decoding order, BS transmit beamforming vector, received PS ratio, and IRS phase shift. This problem is challenging mainly because the changes of wireless channel make the users' decoding order more complicated, and the BS transmit beamforming vector, PS ratio, and IRS phase shift are highly coupled. Therefore, it is necessary to design an effective algorithm for the IRS-assisted SWIPT NOMA networks to minimize the BS transmit power.

Based on the above, the main contributions of this paper can be summarized as follows:

- We propose an IRS-assisted SWIPT NOMA network framework, in which multiple users can share the same resource blocks at the same time, and users can obtain energy while receiving information. In addition, IRS can adjust the channel to improve NOMA performance and WPT efficiency of SWIPT. We formulate the BS transmit power minimization problem for joint optimization of the SIC decoding order, BS transmit beamforming vector, PS ratio, and IRS phase shift. Since the optimization variables are highly coupled, solving this problem is challenging.

- In order to solve the optimization problem, we divide the problem into two stages. Specifically, in the first stage, an SIC decoding order determination algorithm is proposed based on the maximum combined channel gain. In the second stage, we divide the problem into three sub-problems according to the decoding order obtained in the first stage. Firstly, given PS ratio and IRS phase shift, the BS transmit beamforming vector is optimized by applying semidefinite relaxation (SDR) and successive convex optimization (SCA). For the last two feasibility-check problems of PS ratio and IRS phase shift, we efficiently solve them by applying SDR, SCA and Gaussian randomization. Finally, the three sub-problems are iterated alternately until convergence.
- Through numerical simulation, we verified the effectiveness of the proposed joint SIC decoding order, BS transmit beamforming vector, PS ratio, and IRS phase shift optimization algorithm (JDBPR) compared with the baseline algorithm, i.e., it can significantly decrease the BS transmit power. For the IRS-assisted NOMA SWIPT networks, the BS transmit power is significantly lower than the networks without IRS assistance. Meanwhile, the more reflecting elements of the IRS, the smaller the required BS transmit power, which also means that we can reduce the BS transmit power by increasing the number of IRS elements.

The remainder of this paper is organized as follows. Section II elaborates the system model and optimization problem formulation for the IRS-assisted SWIPT NOMA networks. Section III presents the proposed two-stage optimization algorithm for the formulated optimization problem. In Section IV, numerical results demonstrate that our algorithm has good convergence and effectiveness. Finally, the conclusion is given in Section V.

Notations: Scalars are denoted by lower-case letters, while vectors and matrices are represented by bold lower-case letters and bold upper-case letters, respectively. $|x|$ denotes the absolute value of a complex-valued scalar x, and $\|\mathbf{x}\|$ denotes the Euclidean norm of a complex-valued vector $\mathbf{x}$. $diag(\mathbf{x})$ denotes a diagonal matrix whose diagonal elements are the corresponding elements in vector $\mathbf{x}$. For a square matrix $\mathbf{X}$, $\mathrm{Tr}(\mathbf{X})$, $\mathrm{Rank}(\mathbf{X})$, $\mathbf{X}^H$ and $\mathbf{X}_{m,n}$ denote its trace, rank, conjugate transpose and m,n-th entry, respectively, while $\mathbf{X} \succeq 0$ represents that $\mathbf{X}$ is a positive semidefinite matrix. Similarly, for a general matrix $\mathbf{A}$, $\mathrm{Rank}(\mathbf{A})$, $\mathbf{A}^H$ and $\mathbf{A}_{m,n}$ also denote its rank, conjugate transpose and m,n-th entry, respectively. In addition, $\mathbb{C}^{M\times N}$ denotes the space of $M \times N$ complex matrices. $\mathbf{I}_N$ denotes an dentity matrix of size $N \times N$. j denotes the imaginary unit, i.e., $j^2 = -1$. Finally, the distribution of a circularly symmetric complex Gaussian (CSCG) random vector with mean μ and covariance matrix $\mathbf{C}$ is denoted by $\mathcal{CN}(\mu, \mathbf{C})$, and $\sim$ stands for 'distributed as'.

II. System Model and Problem Formulation

A. System Model

In this paper, we consider the downlink transmission in an IRS-assisted SWIPT NOMA network consisting of one BS, one IRS and K users. The set of users is denoted by $\mathcal{K} = \{1, 2, \ldots, K\}$. It can be assumed that the BS is equipped with $N > 1$ uniform linear array (ULA) antennas and each user is equipped with one antenna. The IRS is equipped with M ULA reflecting elements,[1] denoted by $\mathcal{M} = \{1, 2, \ldots, M\}$. A smart controller is equipped at the IRS to coordinate its switching between two working modes, namely the receiving mode for channel estimation and the reflection mode for signal transmission [46]. Since IRS elements are passively reflective, they are passive devices. We consider the use of time-division duplexing (TDD) protocol for uplink and downlink communication. Combined with the reciprocity of the channel, the downlink channel state information (CSI) can be obtained according to the uplink channel estimation. Thus, we assume the CSI of all channels is perfectly known at the BS.[2] Meanwhile, we assume that all channels are quasi-static flat-fading.

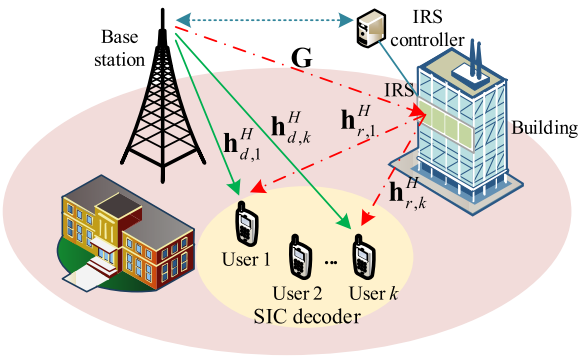

Fig. 1. The IRS-assisted SWIPT NOMA networks.

The channel gains from the BS to IRS, from the IRS to k-th user, and from the BS to k-user are respectively represented by $\mathbf{G} \in \mathbb{C}^{M\times N}$, $\mathbf{h}_{r,k}^H \in \mathbb{C}^{1\times M}$ and $\mathbf{h}_{d,k}^H \in \mathbb{C}^{1\times N}$, $\forall k \in \mathcal{K}$. Let $\mathbf{\Theta} = \mathrm{diag}\left(\beta_1 e^{j\theta_1}, \beta_2 e^{j\theta_2}, \ldots, \beta_M e^{j\theta_M}\right) \in \mathbb{C}^{M\times M}$ denote the reflection coefficients matrix of the IRS, where $\beta_m \in [0, 1]$ and $\theta_m \in [0, 2\pi]$ denote the amplitude reflection coefficient and phase shift of the m-th reflecting element, respectively.[3] Due to the severe path loss, signals reflected by the IRS twice or more are negligible and can be ignored. In the deployment of actual scenarios, we usually consider that the reflecting element of the IRS is designed to maximize the reflected signal, thus $\beta_m = 1, \forall m \in \mathcal{M}$. The wireless channel can be divided into three parts, namely, BS-IRS channel, IRS-user channel, BS-user channel. Although the channel between the

[1]The proposed optimization algorithm when the IRS is equipped with ULA can be well extended to the setup where the IRS is equipped with uniform planar array (UPA).

[2]It is worth noting that although this paper is the design of the optimization algorithm with the assumption that perfect CSI is available at the BS, the framework and process of the proposed optimization algorithm can still be applied to robust optimization algorithm design in the case of imperfect CSI.

[3]It is worth noting that there are IRS amplitude and phase shift models that are closer to the practical system. In order to characterize the basic performance limit of IRS, we assume that the phase shift varies continuously from 0 to 2π. In practice systems, we usually choose from a discrete value from 0 to 2π. Discrete phase shift optimization research will be discussed in the future work. In addition, the amplitude of the IRS can also vary continuously from 0 to 1. In practice, in order to maximize the power of the reflected signal, we usually set $\beta_m = 1$.

BS and users may be blocked, the wireless channel still has a lot of scattering, thus we model the BS-user channel as Rayleigh fading and denote it as $\mathbf{g}_{d,k}^H \in \mathbb{C}^{1\times N}$. We assume that each element of $\mathbf{g}_{d,k}^H$ is independent and identically distributed (i.i.d.) CSCG random variable with zero mean and unit variance. Therefore, the channel gain of the BS-user can be expressed as

$$\mathbf{h}_{d,k}^H = \sqrt{C_0\left(\frac{d_{d,k}}{D_0}\right)^{-\alpha_1}}\mathbf{g}_{d,k}^H, \tag{1}$$

where C_0 represents the path loss when the reference distance $D_0 = 1\,(\mathrm{m})$, $d_{d,k}$ is the distance from the BS to the k-th user, and α_1 represents the path loss exponent.

In addition, for the BS-IRS channel and IRS-user channel, there are LoS components, thus we model them as Rician fading. The BS-IRS channel can be denoted by

$$\bar{\mathbf{G}} = \sqrt{\frac{\kappa}{1+\kappa}}\mathbf{G}^{\mathrm{LoS}} + \sqrt{\frac{1}{1+\kappa}}\mathbf{G}^{\mathrm{NLoS}}, \tag{2}$$

where κ is the Rician factor, $\mathbf{G}^{\mathrm{LoS}} \in \mathbb{C}^{M\times N}$ and $\mathbf{G}^{\mathrm{NLoS}} \in \mathbb{C}^{M\times N}$ are the line-of-sight (LoS) component and non-line-of-sight (NLoS) component, respectively. Each element of $\mathbf{G}^{\mathrm{NLoS}}$ is i.i.d. CSCG random variable with zero mean and unit variance. Similarly, the IRS-user channel can be expressed as

$$\bar{\mathbf{h}}_{r,k}^H = \sqrt{\frac{\vartheta}{1+\vartheta}}\mathbf{h}_{r,k}^{\mathrm{LoS}} + \sqrt{\frac{1}{1+\vartheta}}\mathbf{h}_{r,k}^{\mathrm{NLoS}}, \tag{3}$$

where ϑ is the Rician factor, $\mathbf{h}_{r,k}^{\mathrm{LoS}} \in \mathbb{C}^{1\times M}$ and $\mathbf{h}_{r,k}^{\mathrm{NLoS}} \in \mathbb{C}^{1\times M}$ are the LoS component and NLoS component, respectively. Each element of $\mathbf{h}_{r,k}^{\mathrm{NLoS}}$ is i.i.d. CSCG random variable with zero mean and unit variance.

The LoS component is represented by the array response of ULA. The array response of N elements ULA can be expressed as

$$\mathbf{a}_N(\theta) = \left[1, e^{-j2\pi\frac{d}{\lambda}\sin\theta}, \ldots, e^{-j2\pi(N-1)\frac{d}{\lambda}\sin\theta}\right], \tag{4}$$

where θ represents the angle of arrival (AoA) or angle of departure (AoD) of the signal. Therefore, the LoS component $\mathbf{G}^{\mathrm{LoS}}$ can be given by

$$\mathbf{G}^{\mathrm{LoS}} = \mathbf{a}_M^H(\theta_{\mathrm{AoA},1})\,\mathbf{a}_N(\theta_{\mathrm{AoD},1}), \tag{5}$$

where $\theta_{\mathrm{AoA},1}$ is the AoA to the ULA at the IRS, and $\theta_{\mathrm{AoD},1}$ is the AoD from the ULA at the BS. Similarly, the LoS component $\mathbf{h}_{r,k}^{\mathrm{LoS}}$ can be expressed as

$$\mathbf{h}_{r,k}^{\mathrm{LoS}} = \mathbf{a}_M(\theta_{\mathrm{AoD},2}), \tag{6}$$

where $\theta_{\mathrm{AoD},2}$ is the AoD from the ULA at the IRS.

Therefore, the channel gain of BS-IRS and IRS-user can be expressed as

$$\mathbf{G} = \sqrt{C_0\left(\frac{d_{d,r}}{D_0}\right)^{-\alpha_2}}\bar{\mathbf{G}}, \tag{7}$$

and

$$\mathbf{h}_{r,k}^H = \sqrt{C_0\left(\frac{d_{r,k}}{D_0}\right)^{-\alpha_3}}\bar{\mathbf{h}}_{r,k}^H, \tag{8}$$

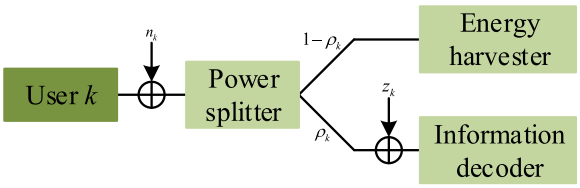

Fig. 2. The PS receiver architecture.

where $d_{d,r}$ and $d_{r,k}$ represent the distance from the BS to the IRS and the distance from the IRS to the k-th user, respectively. α_2 and α_3 respectively represent the path loss exponent from BS to IRS and IRS to the k-th user.

In this paper, we assume linear transmit precoding at BS, where each user is assigned with one dedicated information beam. Therefore, the complex baseband transmitted signal at BS can be expressed as

$$\mathbf{x} = \sum_{k=1}^{K}\mathbf{w}_k s_k, \forall k \in \mathcal{K}, \tag{9}$$

where s_k denotes the transmission data symbol for the k-th user, and $\mathbf{w}_k \in \mathbb{C}^{N\times 1}$ represents the corresponding beamforming vector. We assume that s_k is i.i.d. CSCG random variables with zero mean and unit variance, denoted by $s_k \sim \mathcal{CN}(0,1), \forall k \in \mathcal{K}$.

The received signal at the k-th user from both the BS-user link and BS-IRS-user link can be expressed as

$$y_k = \left(\mathbf{h}_{r,k}^H\boldsymbol{\Theta}\mathbf{G} + \mathbf{h}_{d,k}^H\right)\sum_{j=1}^{K}\mathbf{w}_j s_j + n_k, \forall k \in \mathcal{K}, \tag{10}$$

where $n_k \sim \mathcal{CN}\left(0, \sigma_k^2\right)$ denotes the antenna noise at the k-th user.

In addition, we consider that each user applies PS scheme to coordinate the process of information decoding and energy harvested from the received signal [15]. The PS receiver architecture is shown in Fig. 2. The received signal at each user is split to the information decoder (ID) and the energy harvester (EH) by a power splitter. For the k-th user, it divides $\rho_k\,(0 \le \rho_k \le 1)$ portion of the signal power to the ID, remaining $1-\rho_k$ portion of the signal power to the EH. Therefore, the signal split to the ID for k-th user can be given by

$$y_k^{\mathrm{ID}} = \sqrt{\rho_k}\left(\left(\mathbf{h}_{r,k}^H\boldsymbol{\Theta}\mathbf{G} + \mathbf{h}_{d,k}^H\right)\sum_{j=1}^{K}\mathbf{w}_j s_j + n_k\right) + z_k, \forall k \in \mathcal{K}, \tag{11}$$

where $z_k \sim \mathcal{CN}\left(0, \delta_k^2\right)$ is the additional noise introduced by the ID at the k-th user.

Since we consider NOMA transmission, the SIC decoding order is very important, which is determined by the channel conditions. Unlike the general NOMA communication system, the combination of IRS and NOMA makes the channel more complicated, because the channel gain may change due to the change of the IRS phase shift matrix. Let $s(k)$ denote the decoding order for the k-th user. Then, $s(k) = i$ denotes that the k-th user is the i-th signal to be decoded at the

receiver. Accordingly, the signal to interference-plus-noise-ratio (SINR) of the k-th user can be expressed as

$$\mathrm{SINR}_k = \frac{\rho_k \left| \left(\mathbf{h}_{r,k}^H \mathbf{\Theta} \mathbf{G} + \mathbf{h}_{d,k}^H \right) \mathbf{w}_k \right|^2}{\rho_k \sum\limits_{s(j)>s(k)} \left| \left(\mathbf{h}_{r,k}^H \mathbf{\Theta} \mathbf{G} + \mathbf{h}_{d,k}^H \right) \mathbf{w}_j \right|^2 + \rho_k \sigma_k^2 + \delta_k^2}. \tag{12}$$

It is assumed that $s(k) \leq s\left(\bar{k}\right)$, the SINR of the $\bar{k}$-th user decoding information signal of the k-th user can be given by

$$\mathrm{SINR}_{\bar{k}\to k} = \frac{\rho_{\bar{k}} \left| \left(\mathbf{h}_{r,\bar{k}}^H \mathbf{\Theta} \mathbf{G} + \mathbf{h}_{d,\bar{k}}^H \right) \mathbf{w}_k \right|^2}{\rho_{\bar{k}} \sum\limits_{s(j)>s(k)} \left| \left(\mathbf{h}_{r,\bar{k}}^H \mathbf{\Theta} \mathbf{G} + \mathbf{h}_{d,\bar{k}}^H \right) \mathbf{w}_j \right|^2 + \rho_{\bar{k}} \sigma_{\bar{k}}^2 + \delta_{\bar{k}}^2}. \tag{13}$$

In order to ensure that the $\bar{k}$-th user can decode the information of the k-th user with the decoding order $s(k) \leq s\left(\bar{k}\right)$, the SIC decoding condition $\mathrm{SINR}_k \leq \mathrm{SINR}_{\bar{k}\to k}$ should be satisfied [47]. For example, supposing the decoding order of the three users is $s(k) = i, i = 1, 2, 3$. Therefore, the SIC decoding conditions at user 2 and user 3 should satisfy the following conditions: $\mathrm{SINR}_{2\to 1} \geq \mathrm{SINR}_1$, $\mathrm{SINR}_{3\to 1} \geq \mathrm{SINR}_1$ and $\mathrm{SINR}_{3\to 2} \geq \mathrm{SINR}_2$.

In addition, the signal split to the EH for the k-th user can be expressed as

$$y_k^{\mathrm{EH}} = \sqrt{1-\rho_k} \left(\left(\mathbf{h}_{r,k}^H \mathbf{\Theta} \mathbf{G} + \mathbf{h}_{d,k}^H \right) \sum_{j=1}^{K} \mathbf{w}_j s_j + n_k \right), \tag{14}$$

Then, the harvested power by the EH for the k-th user can be given by

$$E_k = \eta_k \left(1-\rho_k\right) \left(\sum_{j=1}^{K} \left| \left(\mathbf{h}_{r,k}^H \mathbf{\Theta} \mathbf{G} + \mathbf{h}_{d,k}^H \right) \mathbf{w}_j \right|^2 + \sigma_k^2 \right), \tag{15}$$

where $\eta_k \in (0, 1]$ denotes the power conversion efficiency at EH of the k-th user. In this paper, we consider the normalized time, then the harvested power is the harvested energy.

B. Problem Formulation for the IRS-Assisted SWIPT NOMA Networks

In this paper, we aim to minimize the BS transmit power by jointly designing SIC decoding order, BS transmit beamforming vector, received PS ratio and IRS phase shift matrix. Accordingly, the problem can be formulated as follows,

$$(\mathrm{P1}) \min_{\{\mathbf{w}_k, \theta_m, \rho_k, s(k)\}} \sum_{k=1}^{K} \|\mathbf{w}_k\|^2, \tag{16a}$$

$$\mathrm{s.t.} \ \frac{\rho_{\mathrm{k}} \left| \left(\mathbf{h}_{\mathrm{r,k}}^{\mathrm{H}} \mathbf{\Theta} \mathbf{G} + \mathbf{h}_{\mathrm{d,k}}^{\mathrm{H}} \right) \mathbf{w}_{\mathrm{k}} \right|^2}{\rho_{\mathrm{k}} \sum\limits_{\mathrm{s(j)>s(k)}} \left| \left(\mathbf{h}_{\mathrm{r,k}}^{\mathrm{H}} \mathbf{\Theta} \mathbf{G} + \mathbf{h}_{\mathrm{d,k}}^{\mathrm{H}} \right) \mathbf{w}_{\mathrm{j}} \right|^2 + \rho_{\mathrm{k}} \sigma_{\mathrm{k}}^2 + \delta_{\mathrm{k}}^2} \geq \gamma_{\mathrm{k}}, \tag{16b}$$

$$\mathrm{SINR}_k \leq \mathrm{SINR}_{\bar{k}\to k}, \ \text{if} \ s(k) \leq s\left(\bar{k}\right), \tag{16c}$$

$$\eta_k \left(1-\rho_k\right) \left(\sum_{j=1}^{K} \left| \left(\mathbf{h}_{r,k}^H \mathbf{\Theta} \mathbf{G} + \mathbf{h}_{d,k}^H \right) \mathbf{w}_j \right|^2 + \sigma_k^2 \right) \geq e_k, \tag{16d}$$

$$0 \leq \rho_k \leq 1, \tag{16e}$$

$$0 \leq \theta_m \leq 2\pi, \tag{16f}$$

$$s(k) \in \Omega, \tag{16g}$$

where constraint (16b) guarantees the QoS requirement of the k-th user with the SINR threshold γ_k. Meanwhile, constraint (16c) ensures SIC decoding conditions. In addition, constraint (16d) requires that the energy harvested of the k-th user needs to reach a threshold e_k. Considering that each user should have non-zero SINR threshold and energy harvested threshold, i.e., $\gamma_k > 0$ and $e_k > 0$, the received PS ratio of the k-th user should satisfy constraint (16e). Constraint (16f) is the condition that IRS phase shift should meet. Ω in constraint (16g) is the combination set of all possible SIC decoding orders.

It can be seen that the problem (P1) is a non-convex optimization problem due to the following reasons. Firstly, the BS transmit beamforming, received PS ratio and IRS phase shift matrix are highly coupled. In addition, the phase shift is expressed in exponential form. Finally, the SIC decoding orders are determined by the IRS phase shift, thus the SIC decoding order and the IRS phase shift are also related. Therefore, it is challenging to directly solve this problem.

III. The Proposed Two-Stage Optimization Algorithm for the IRS-Assisted SWIPT NOMA Networks

In this section, we propose a two-stage optimization algorithm to solve the problem (P1). The problem (P1) is decoupled into two stages. Firstly, an SIC decoding order determination algorithm based on combined channel gain is proposed. Then, for the given SIC decoding order, the beamforming vector, PS ratio and IRS phase shift matrix are alternately optimized by applying SDR, SCA and Gaussian randomization.

A. SIC Decoding Order Determination Algorithm

In this subsection, the SIC decoding order determination algorithm based on the combined channel gains is proposed. Since this paper considers NOMA, the SIC decoding order is a factor that must be considered. In fact, the SIC decoding order is determined by the channel gain from the BS to each user. Due to the addition of IRS, the SIC decoding order is not only determined by the direct channel gain from the BS to the ground user, but by the combined channel gain from the BS to each user. The change of the IRS phase shift matrix will influence the combined channel gain. Since the same phase shift is different for all users, the combined channel gain of different users cannot be maximized at the same time. Therefore, we maximize sum of the combined channel gain from the BS to all users by optimizing the IRS phase shift. We can sort the combined channel gains of all users to determine the SIC decoding order. The problem of

maximizing the sum of the combined channel gains of all users can be expressed as

$$\text{(P2)} \quad \max_{\mathbf{\Theta}} \sum_{k=1}^{K} \left\|\mathbf{h}_{r,k}^{H}\mathbf{\Theta}\mathbf{G}+\mathbf{h}_{d,k}^{H}\right\|^{2}, \tag{17a}$$

$$\text{s.t. } 0 \le \theta_{\mathrm{m}} \le 2\pi, \tag{17b}$$

where $\mathbf{\Theta} = \operatorname{diag}\left(e^{j\theta_1}, e^{j\theta_2}, \ldots, e^{j\theta_M}\right)$. Let $u_m = e^{j\theta_m}, \forall m \in \mathcal{M}$, $\mathbf{u} = [u_1, u_2, \ldots, u_M]^H \in \mathbb{C}^{M\times 1}$. Then the constraint on θ_m is equivalent to $|u_m| = 1, \forall m \in \mathcal{M}$. Let $\mathbf{a}_k = \operatorname{diag}\left(\mathbf{h}_{r,k}^{H}\right)\mathbf{G} \in \mathbb{C}^{M\times N}$, then $\left\|\mathbf{h}_{r,k}^{H}\mathbf{\Theta}\mathbf{G}+\mathbf{h}_{d,k}^{H}\right\|^{2}$ can be written as $\left\|\mathbf{u}^{H}\mathbf{a}_k+\mathbf{h}_{d,k}^{H}\right\|^{2}$. We introduce auxiliary variables as follows,

$$\mathbf{R}_k = \begin{bmatrix} \mathbf{a}_k\mathbf{a}_k^{H} & \mathbf{a}_k\mathbf{h}_{d,k} \\ \mathbf{h}_{d,k}^{H}\mathbf{a}_k^{H} & 0 \end{bmatrix}, \bar{\mathbf{u}} = \begin{bmatrix} \mathbf{u} \\ 1 \end{bmatrix}. \tag{18}$$

Therefore, $\left\|\mathbf{u}^{H}\mathbf{a}_k+\mathbf{h}_{d,k}^{H}\right\|^{2}$ can be further expressed as $\bar{\mathbf{u}}^{H}\mathbf{R}_k\bar{\mathbf{u}}+\left\|\mathbf{h}_{d,k}^{H}\right\|^{2}$. Since $\bar{\mathbf{u}}^{H}\mathbf{R}_k\bar{\mathbf{u}} = \operatorname{Tr}\left(\mathbf{R}_k\bar{\mathbf{u}}\bar{\mathbf{u}}^{H}\right)$, we define $\bar{\mathbf{U}} = \bar{\mathbf{u}}\bar{\mathbf{u}}^{H}$, where $\bar{\mathbf{U}} \succeq 0$ and $\operatorname{Rank}\left(\bar{\mathbf{U}}\right) = 1$. Since the rank-one constraint is non-convex, we use SDR to relax this constraint firstly, and the problem (P2) can be transformed into

$$\text{(P2.1)} \quad \max_{\bar{\mathbf{U}}} \sum_{k=1}^{K} \left(\operatorname{Tr}\left(\mathbf{R}_k\bar{\mathbf{U}}\right)+\left\|\mathbf{h}_{d,k}^{H}\right\|^{2}\right), \tag{19a}$$

$$\text{s.t. } \bar{\mathbf{U}}_{\mathrm{m,m}} = 1, \mathrm{m} = 1, 2, \ldots, \mathrm{M}+1, \tag{19b}$$

$$\bar{\mathbf{U}} \succeq 0. \tag{19c}$$

The above problem (P2.1) is a standard semidefinite programming (SDP) problem, which can be solved by using CVX toolbox [48]. The problem (P2.1) is equivalent to the problem (P2) if and only if the optimal solution $\bar{\mathbf{U}}^{*}$ of the problem (P2.1) is a rank-one matrix. However, under normal circumstances, the problem (P2.1) generally does not produce a rank-one solution, i.e., $\operatorname{Rank}\left(\bar{\mathbf{U}}\right) \neq 1$. The optimal solution of problem (P2.1) is only the upper bound of problem (P2), so it is necessary to reconstruct the high-rank solution obtained from problem (P2.1) into a rank-one solution. In this paper, we use Gaussian randomization to reduce the rank of high-rank solution. Since $\operatorname{Rank}\left(\bar{\mathbf{U}}\right) \neq 1$, the eigenvalue decomposition of $\bar{\mathbf{U}}$ can be expressed as

$$\bar{\mathbf{U}} = \mathbf{V}\mathbf{\Sigma}\mathbf{V}^{H}, \tag{20}$$

where $\mathbf{V} = [e_1, e_2, \ldots, e_{M+1}]$ is the identity matrix of the eigenvector, and $\mathbf{\Sigma} = \operatorname{diag}\left(\lambda_1, \lambda_2, \ldots, \lambda_{M+1}\right)$ is the diagonal matrix of the eigenvalue. Next, we generate two independent zero-mean normal distribution random vectors $\alpha \in \mathbb{R}^{(M+1)\times 1}$, $\beta \in \mathbb{R}^{(M+1)\times 1}$ and covariance matrix $\frac{1}{2}\mathbf{I}_{M+1}$. Let T be the maximum generation of candidate random variables. The Gaussian random vector of the t-th generation can be expressed as

$$\mathbf{r}_t = \alpha_t + \beta_t\sqrt{-1}, t = 1, 2, \ldots, T, \tag{21}$$

where $\alpha_{\mathbf{t}}$ and $\beta_{\mathbf{t}}$ are the t-th generation random vectors. Based on the obtained Gaussian random vector $\mathbf{r}_t \sim \mathcal{CN}\left(\mathbf{0}, \mathbf{I}_{M+1}\right)$, we can obtain the suboptimal solution of the problem (P2.1), which can be expressed as

$$\bar{\mathbf{u}}_t = \mathbf{V}\mathbf{\Sigma}^{1/2}\mathbf{r}_t, t = 1, 2, \ldots, T. \tag{22}$$

Therefore, the candidate reflection matrix can be expressed as

$$\mathbf{\Theta}_t = \operatorname{diag}\left(e^{j\arg\left(\frac{\bar{\mathbf{u}}_t[m]}{\bar{\mathbf{u}}_t[M+1]}\right)}\middle|\, \forall m \in \mathcal{M}\right), \tag{23}$$

where $\bar{\mathbf{u}}_t[m]$ represents the m-th reflecting element of $\bar{\mathbf{u}}_t$. According to the obtained candidate reflection matrix set $\{\mathbf{\Theta}_t | \, t = 1, 2, \ldots, T\}$, we can obtain the one that maximizes the combined channel gain of all users, i.e.,

$$t^{*} = \arg\max_{t} \sum_{k=1}^{K} \left\|\mathbf{h}_{r,k}^{H}\mathbf{\Theta}_t\mathbf{G}+\mathbf{h}_{d,k}^{H}\right\|^{2}. \tag{24}$$

It has been verified that SDR technique followed by such randomization scheme can guarantee at least a $\pi/4$-approximation of the optimal objective value of the problem (P2) [17].

B. BS Beamforming Vector Optimization

Let $\mathbf{h}_k^{H} = \mathbf{h}_{r,k}^{H}\mathbf{\Theta}\mathbf{G}+\mathbf{h}_{d,k}^{H} \in \mathbb{C}^{1\times N}$. Based on the SIC decoding order obtained in the first stage, and given PS ratio IRS phase shift, the problem (P1) can be transformed into the problem (P3), which can be expressed as

$$\text{(P3)} \quad \min_{\{\mathbf{w}_k\}} \sum_{k=1}^{K} \|\mathbf{w}_k\|^{2}, \tag{25a}$$

$$\text{s.t. } \frac{\rho_{\mathrm{k}}\left|\mathbf{h}_{\mathrm{k}}^{\mathrm{H}}\mathbf{w}_{\mathrm{k}}\right|^{2}}{\rho_{\mathrm{k}}\sum\limits_{\mathrm{s(j)>s(k)}}\left|\mathbf{h}_{\mathrm{k}}^{\mathrm{H}}\mathbf{w}_{\mathrm{j}}\right|^{2}+\rho_{\mathrm{k}}\sigma_{\mathrm{k}}^{2}+\delta_{\mathrm{k}}^{2}} \ge \gamma_{\mathrm{k}}, \tag{25b}$$

$$\frac{\rho_k\left|\mathbf{h}_k^{H}\mathbf{w}_k\right|^{2}}{\rho_k\sum\limits_{s(j)>s(k)}\left|\mathbf{h}_k^{H}\mathbf{w}_j\right|^{2}+\rho_k\sigma_k^{2}+\delta_k^{2}} \le \frac{\rho_{\bar{k}}\left|\mathbf{h}_{\bar{k}}^{H}\mathbf{w}_k\right|^{2}}{\rho_{\bar{k}}\sum\limits_{s(j)>s(k)}\left|\mathbf{h}_{\bar{k}}^{H}\mathbf{w}_j\right|^{2}+\rho_{\bar{k}}\sigma_{\bar{k}}^{2}+\delta_{\bar{k}}^{2}}, \text{ if } s(k) < s\left(\bar{k}\right), \tag{25c}$$

$$\eta_k\left(1-\rho_k\right)\left(\sum_{j=1}^{K}\left|\mathbf{h}_k^{H}\mathbf{w}_j\right|^{2}+\sigma_k^{2}\right) \ge e_k. \tag{25d}$$

Define $\mathbf{W}_k = \mathbf{w}_k\mathbf{w}_k^{H} \in \mathbb{C}^{N\times N}, \forall k$, and $\mathbf{W}_k$ satisfies $\operatorname{Rank}\left(\mathbf{W}_k\right) = 1, \forall k$. We first apply SDR to relax the rank-one constraint, the problem (P3) can be transformed into the problem (P3.1), which can be expressed as

$$\text{(P3.1)} \quad \min_{\{\mathbf{W}_k\}} \sum_{k=1}^{K} \operatorname{Tr}\left(\mathbf{W}_k\right), \tag{26a}$$

$$\text{s.t. } \frac{\mathbf{h}_{\mathrm{k}}^{\mathrm{H}}\mathbf{W}_{\mathrm{k}}\mathbf{h}_{\mathrm{k}}}{\sum\limits_{\mathrm{s(j)>s(k)}}\mathbf{h}_{\mathrm{k}}^{\mathrm{H}}\mathbf{W}_{\mathrm{j}}\mathbf{h}_{\mathrm{k}}+\sigma_{\mathrm{k}}^{2}+\frac{\delta_{\mathrm{k}}^{2}}{\rho_{\mathrm{k}}}} \ge \gamma_{\mathrm{k}}, \tag{26b}$$

$$\frac{\mathbf{h}_k^{H}\mathbf{W}_k\mathbf{h}_k}{\sum\limits_{s(j)>s(k)}\mathbf{h}_k^{H}\mathbf{W}_j\mathbf{h}_k+\sigma_k^{2}+\frac{\delta_k^{2}}{\rho_k}} \le$$

$$\frac{\mathbf{h}_{\bar{k}}^H \mathbf{W}_k \mathbf{h}_{\bar{k}}}{\sum\limits_{s(j)>s(k)} \mathbf{h}_{\bar{k}}^H \mathbf{W}_j \mathbf{h}_{\bar{k}} + \sigma_{\bar{k}}^2 + \frac{\delta_{\bar{k}}^2}{\rho_{\bar{k}}}}, \text{ if } s(k) < s\left(\bar{k}\right), \quad (26c)$$

$$\eta_k \left(1-\rho_k\right) \left(\sum_{j=1}^{K} \mathbf{h}_k^H \mathbf{W}_j \mathbf{h}_k + \sigma_k^2 \right) \geq e_k, \quad (26d)$$

$$\mathbf{W}_k \succeq 0. \quad (26e)$$

Since the constraint (26c) is non-convex, the problem (P3.1) is still a non-convex optimization problem. In this paper, we use SCA to convert the constraint (26c) into

$$\hat{f}_1\left(\mathbf{W}_k\right) - \ln\left(\sum_{s(j)>s(k)} \mathbf{h}_k^H \mathbf{W}_j \mathbf{h}_k + A_k \right) - \ln\left(\mathbf{h}_{\bar{k}}^H \mathbf{W}_k \mathbf{h}_{\bar{k}}\right) + \hat{f}_2\left(\mathbf{W}_j\right) \leq 0, \text{ if } s(k) < s\left(\bar{k}\right), \quad (27)$$

where $\mathbf{W}_k^{(r)}$ is the value of $\mathbf{W}_k$ for the r-th iteration. See Appendix A for $\hat{f}_1\left(\mathbf{W}_k\right)$ and $\hat{f}_2\left(\mathbf{W}_j\right)$.

Please refer to Appendix A for the detailed proof. ■

Accordingly, the problem (P3.1) can be transformed into the problem (P3.2), which can be expressed as

$$\text{(P3.2)} \quad \min_{\{\mathbf{W}_k\}} \sum_{k=1}^{K} \mathrm{Tr}\left(\mathbf{W}_k\right), \quad (28a)$$

$$\text{s.t. (26b), (27), (26d), (26e).} \quad (28b)$$

The problem (P3.2) is a standard SDP problem, which can be solved by applying the CVX toolbox [48]. We assume that $\mathbf{W}_k^*$ is the optimal solution of the problem (P3.2). If $\mathbf{W}_k^*$ satisfies $\mathrm{Rank}\left(\mathbf{W}_k^*\right) = 1, \forall k$, the beamforming vector $\mathbf{w}_k^*$ of the problem (P3) can be obtained by eigenvalue decomposition. Next, we have the following proposition.

Proposition 1: The optimal solution $\mathbf{W}_k^*$ of the problem (P3.2) satisfies $\mathrm{Rank}\left(\mathbf{W}_k^*\right) = 1, \forall k$, i.e., the SDR for the problem (P3) is tight.

Please refer to Appendix B for the detailed proof. ■

C. PS Ratio Optimization

In this sub-problem, according to the SIC decoding order obtained in the first stage, given BS beamforming vector and IRS phase shift, the problem (P1) can be transformed into a feasibility-check problem (P4), which can be given by

$$\text{(P4)} \quad \text{find} \quad \rho_k, \quad (29a)$$

$$\text{s.t.} \quad \frac{\rho_{\mathrm{k}} \left|\mathbf{h}_{\mathrm{k}}^{\mathrm{H}} \mathbf{w}_{\mathrm{k}}\right|^2}{\rho_{\mathrm{k}} \left(\sum\limits_{\mathrm{s(j)>s(k)}} \left|\mathbf{h}_{\mathrm{k}}^{\mathrm{H}} \mathbf{w}_{\mathrm{j}}\right|^2 + \sigma_{\mathrm{k}}^2 \right) + \delta_{\mathrm{k}}^2} \geq \gamma_{\mathrm{k}}, \quad (29b)$$

$$\frac{\rho_k \left|\mathbf{h}_k^H \mathbf{w}_k\right|^2}{\rho_k \left(\sum\limits_{s(j)>s(k)} \left|\mathbf{h}_k^H \mathbf{w}_j\right|^2 + \sigma_k^2 \right) + \delta_k^2} \leq \frac{\rho_{\bar{k}} \left|\mathbf{h}_{\bar{k}}^H \mathbf{w}_k\right|^2}{\rho_{\bar{k}} \left(\sum\limits_{s(j)>s(k)} \left|\mathbf{h}_{\bar{k}}^H \mathbf{w}_j\right|^2 + \sigma_{\bar{k}}^2 \right) + \delta_{\bar{k}}^2}, \text{if } s(k) < s\left(\bar{k}\right), \quad (29c)$$

$$\eta_k \left(1-\rho_k\right) \left(\sum_{j=1}^{K} \left|\mathbf{h}_k^H \mathbf{w}_j\right|^2 + \sigma_k^2 \right) \geq e_k, \quad (29d)$$

$$0 \leq \rho_k \leq 1. \quad (29e)$$

Due to the existence of the non-convex constraint (29c), the problem (P4) is a non-convex optimization problem. By applying SCA, the constraint (29c) is transformed into

$$\frac{B_{kk}\delta_{\bar{k}}^2}{\rho_{\bar{k}}} - B_{\bar{k}k}\delta_k^2 \left(\frac{1}{\rho_k^{(r)}} - \frac{1}{\left(\rho_k^{(r)}\right)^2} \left(\rho_k - \rho_k^{(r)}\right) \right) \leq B_{\bar{k}k} B_{jk} - B_{kk} B_{j\bar{k}}, \text{ if } s(k) < s\left(\bar{k}\right), \quad (30)$$

where $\rho_k^{(r)}$ is the value of ρ_k for the r-th iteration.

Please refer to the Appendix C for detailed proof. ■

Thus, the problem (P4) can be rewritten as

$$\text{(P4.1)} \quad \text{find} \quad \rho_k, \quad (31a)$$

$$\text{s.t. (29b), (30), (29d), (29e).} \quad (31b)$$

It can be seen that the problem (P4.1) is a standard convex optimization problem, which can be solved by applying the CVX toolbox [48].

D. IRS Phase Shift Optimization

When the SIC decoding order is determined, and beamforming vector and PS ratio are fixed, according to the variable substitution $\mathbf{u}=\left[e^{j\theta_1}, \ldots, e^{j\theta_M}\right]^H \in \mathbb{C}^{M\times 1}$ in Section III.A, the constraint on θ_m can be transformed into $|u_m| = 1, \forall m \in \mathcal{M}$. Let $\mathbf{p}_{k,j} = \mathrm{diag}\left(\mathbf{h}_{r,j}^H\right) \mathbf{G} \mathbf{w}_k \in \mathbb{C}^{M\times 1}$, $\mathbf{q}_{k,j} = \mathbf{h}_{d,j}^H \mathbf{w}_k \in \mathbb{C}$. Then $\left| \left(\mathbf{h}_{r,j}^H \mathbf{\Theta} \mathbf{G} + \mathbf{h}_{d,j}^H\right) \mathbf{w}_k \right|^2 = \left|\mathbf{u}^H \mathbf{p}_{k,j} + \mathbf{q}_{k,j}\right|^2$. Next we introduce auxiliary variables as follows,

$$\mathbf{S}_{k,j} = \begin{bmatrix} \mathbf{p}_{k,j}\mathbf{p}_{k,j}^H & \mathbf{p}_{k,j}\mathbf{q}_{k,j}^H \\ \mathbf{q}_{k,j}\mathbf{p}_{k,j}^H & 0 \end{bmatrix}, \bar{\mathbf{u}} = \begin{bmatrix} \mathbf{u} \\ 1 \end{bmatrix}. \quad (32)$$

Then $\left|\mathbf{u}^H \mathbf{p}_{k,j} + \mathbf{q}_{k,j}\right|^2 = \bar{\mathbf{u}}^H \mathbf{S}_{k,j} \bar{\mathbf{u}} + |\mathbf{q}_{k,j}|^2$. Since $\bar{\mathbf{u}}^H \mathbf{S}_{k,j} \bar{\mathbf{u}} = \mathrm{Tr}\left(\mathbf{S}_{k,j} \bar{\mathbf{u}} \bar{\mathbf{u}}^H\right)$, we define $\bar{\mathbf{U}} = \bar{\mathbf{u}} \bar{\mathbf{u}}^H$, where $\bar{\mathbf{U}}$ satisfies $\bar{\mathbf{U}} \succeq 0$ and $\mathrm{Rank}\left(\bar{\mathbf{U}}\right) = 1$. Since rank-one constraint is non-convex constraint, we firstly apply the SDR to relax it. Because the objective function of the problem (P1) does not contain the IRS phase shift variable, the problem (P1) is transformed into a feasibility-check problem (P5), which can be expressed as

$$\text{(P5)} \quad \text{find} \quad \bar{\mathbf{U}}, \quad (33a)$$

$$\text{s.t.} \quad \frac{\mathrm{Tr}\left(\mathbf{S}_{\mathrm{k,k}} \bar{\mathbf{U}}\right) + |\mathbf{q}_{\mathrm{k,k}}|^2}{\sum\limits_{\mathrm{s(j)>s(k)}} \left(\mathrm{Tr}\left(\mathbf{S}_{\mathrm{j,k}} \bar{\mathbf{U}}\right) + |\mathbf{q}_{\mathrm{j,k}}|^2 \right) + \sigma_{\mathrm{k}}^2 + \frac{\delta_{\mathrm{k}}^2}{\rho_{\mathrm{k}}}} \geq \gamma_{\mathrm{k}}, \quad (33b)$$

$$\frac{\mathrm{Tr}\left(\mathbf{S}_{k,k} \bar{\mathbf{U}}\right) + |\mathbf{q}_{k,k}|^2}{\sum\limits_{s(j)>s(k)} \left(\mathrm{Tr}\left(\mathbf{S}_{j,k} \bar{\mathbf{U}}\right) + |\mathbf{q}_{j,k}|^2 \right) + \sigma_k^2 + \frac{\delta_k^2}{\rho_k}} \leq \frac{\mathrm{Tr}\left(\mathbf{S}_{k,\bar{k}} \bar{\mathbf{U}}\right) + \left|\mathbf{q}_{k,\bar{k}}\right|^2}{\sum\limits_{s(j)>s(k)} \left(\mathrm{Tr}\left(\mathbf{S}_{j,\bar{k}} \bar{\mathbf{U}}\right) + \left|\mathbf{q}_{j,\bar{k}}\right|^2 \right) + \sigma_{\bar{k}}^2 + \frac{\delta_{\bar{k}}^2}{\rho_{\bar{k}}}}, \quad (33c)$$

$$\mathrm{Tr}\left(\mathbf{R}_k \bar{\mathbf{U}}\right) + \left\|\mathbf{h}_{d,k}^H\right\|^2 \leq \mathrm{Tr}\left(\mathbf{R}_{\bar{k}} \bar{\mathbf{U}}\right) + \left\|\mathbf{h}_{d,\bar{k}}^H\right\|^2, \quad (33d)$$

$$\eta_k\left(1-\rho_k\right)\left(\sum_{j=1}^{K}\mathrm{Tr}\left(\mathbf{S}_{j,k}\bar{\mathbf{U}}\right)+\left|\mathbf{q}_{j,k}\right|^2+\sigma_k^2\right)\geq e_k, \tag{33e}$$

$$\bar{\mathbf{U}}_{m,m}=1, m=1,2,\ldots,M+1, \tag{33f}$$

$$\bar{\mathbf{U}}\succeq 0. \tag{33g}$$

We apply SCA to transform the non-convex constraint (33c) into

$$\hat{g}_1\left(\bar{\mathbf{U}}\right)-\ln\left(\sum_{s(j)>s(k)}\left(\mathrm{Tr}\left(\mathbf{S}_{j,k}\bar{\mathbf{U}}\right)+\left|\mathbf{q}_{j,k}\right|^2\right)+C_k\right)-\ln\left(\mathrm{Tr}\left(\mathbf{S}_{k,\bar{k}}\bar{\mathbf{U}}\right)+\left|\mathbf{q}_{k,\bar{k}}\right|^2\right)+\hat{g}_2\left(\bar{\mathbf{U}}\right)\leq 0, \tag{34}$$

where $\bar{\mathbf{U}}^{(r)}$ is the value of $\bar{\mathbf{U}}$ for the r-th iteration. See Appendix D for $\hat{g}_1\left(\bar{\mathbf{U}}\right)$ and $\hat{g}_2\left(\bar{\mathbf{U}}\right)$.

Please refer to Appendix D for the detailed proof. ■

Thus, the problem (P5) can be transformed into the problem (P5.1), which can be expressed as

$$(\text{P5.1})\ \text{find}\ \bar{\mathbf{U}}, \tag{35a}$$

$$\text{s.t. (33b), (34), (33d), (33e), (33f), (33g).} \tag{35b}$$

The problem (P5.1) is a standard SDP programming problem, which can be solved by CVX toolbox [48]. In general, problem (P5.1) does not produce a rank-one solution, i.e., $\mathrm{Rank}\left(\mathbf{U}\right)\neq 1$. The optimal solution obtained by the problem (P5.1) is only the upper bound of the optimal solution. Therefore, it is necessary to reconstruct the high-rank solution obtained in problem (P5.1) into a rank-one solution, i.e., to reduce the rank of the high-rank solution by using the Gaussian randomization in the subsection III.A.

E. Two-Stage Overall Optimization Algorithm

Based on the previous sub-sections, the two-stage overall optimization algorithm is summarized as **Algorithm 1** (i.e. JDBPR algorithm). Specifically, in the first stage, the SIC decoding order is determined by solving the problem (P2), which mainly optimizes the IRS phase shift matrix to maximize the combined channel gain of all users, and then determines the decoding order according to the combined channel gain of each user. Based on the SIC decoding order obtained in the first stage, when PS ratio and IRS phase shift are fixed in the second stage, the BS beamforming vector is obtained by solving the problem (P3) by applying SDR and SCA, and SDR is proved tight. Next, the last two sub-problems of PS ratio and IRS phase shift can be obtained by solving problem (P4) and (P5) by using SDR, SCA and Gaussian randomization when BS transmit beamforming vector is given. The three sub-problems of the second stage are alternately optimized to achieve convergence[4]

[4]For the two-stage overall optimization algorithm (i.e., JDBPR algorithm) proposed in this paper, the Gaussian randomization used in the first stage can obtain an approximate value of at least $\pi/4$ for the optimal objective value of this stage. Meanwhile, for the three sub-problems of the second stage, since each of the three sub-problems has a complex SIC decoding condition constraint, we apply SCA to solve these sub-problems. Therefore, the JDBPR algorithm can obtain a sub-optimal solution of the problem (P1).

Algorithm 1 Two-Stage **J**oint SIC **D**ecoding Order, BS Transmit **B**eamforming Vector, **P**S Ratio and **I**RS Phase Shift Optimization (JDBPR) Algorithm

1: **Stage 1:** SIC decoding order determination.
2: Obtain the SIC decoding order $\{s(k)\}$ by solving the problem (P2.1).
3: **Stage 2:** Joint BS transmit beamforming vector, PS ratio and IRS phase shift optimization.
4: Initialize $\{\mathbf{w}_k\}^{(0)}$, $\{\rho_k\}^{(0)}$ and $\{\theta_m\}^{(0)}$. Let $r=0$, $\varepsilon=10^{-3}$.
5: **repeat**
6: Solve the problem (P3.2) for given $\{\rho_k\}^{(r)}$ and $\{\theta_m\}^{(r)}$, and obtain BS transmit beamforming vector $\{\mathbf{w}_k\}^{(r+1)}$.
7: Solve the problem (P4.1) for given $\{\mathbf{w}_k\}^{(r+1)}$ and $\{\theta_m\}^{(r)}$, and obtain PS ratio $\{\rho_k\}^{(r+1)}$.
8: Solve the problem (P5.1) for given $\{\mathbf{w}_k\}^{(r+1)}$ and $\{\rho_k\}^{(r+1)}$, and obtain IRS phase shift $\{\theta_m\}^{(r+1)}$.
9: Update $r=r+1$.
10: **until** The fractional decrease of the objective value is below a threshold ε.
11: **return** SIC decoding order, BS transmit beamforming vector, PS ratio and IRS phase shift.

F. Computational Complexity and Convergence Analysis of the Proposed JDBPR Algorithm

1) Computational Complexity Analysis: In each iteration, since both problem (P2.1) and (5.1) optimize the IRS phase shift, they both solve a relaxed SDP problem by interior point method, so the computational complexity of problem (P2.1) and (5.1) in solving the SDP problem can be represented by $\mathcal{O}\left(\left(M+1\right)^{3.5}\right)$. The computational complexity of using the interior point method to solve the problem (P3.2) is $\mathcal{O}\left(KN^{3.5}\right)$ [49], and the problem (P4.1) is solved with the complexity of $\mathcal{O}\left(K\right)$. We assume that the number of iterations required for the algorithm to reach convergence is r, the computational complexity of the proposed JDBPR algorithm can be expressed as $\mathcal{O}\left(r\left(KN^{3.5}+\left(M+1\right)^{3.5}+K\right)\right)$.

2) Convergence Analysis: The convergence of the proposed two-stage JDBPR algorithm mainly lies in the second stage because the first stage only determines the decoding order. Therefore, the convergence performance of the second-stage problem needs to be proved as follows.

We define $\{\mathbf{w}_k\}^{(r)}$, $\{\rho_k\}^{(r)}$ and $\{\theta_m\}^{(r)}$ as the r-th iteration solution of the problem (P3.2), (P4.1) and (P5.1). The objective function is denoted by $\mathcal{P}\left(\{\mathbf{w}_k\}^{(r)},\{\rho_k\}^{(r)},\{\theta_m\}^{(r)}\right)$. In the step 6 of **Algorithm 1**, since BS transmit beamforming vector can be obtained for given $\{\rho_k\}^{(r)}$ and $\{\theta_m\}^{(r)}$. Hence, we have

$$\mathcal{P}\left(\{\mathbf{w}_k\}^{(r)},\{\rho_k\}^{(r)},\{\theta_m\}^{(r)}\right)\geq\mathcal{P}\left(\{\mathbf{w}_k\}^{(r+1)},\{\rho_k\}^{(r)},\{\theta_m\}^{(r)}\right). \tag{36}$$

In the step 7 of **Algorithm 1**, we can obtain PS ratio when $\{\mathbf{w}_k\}^{(r+1)}$ and $\{\theta_m\}^{(r)}$ are given. Herein, we also have

$$\mathcal{P}\left(\{\mathbf{w}_k\}^{(r+1)}, \{\rho_k\}^{(r)}, \{\theta_m\}^{(r)}\right) \geq \mathcal{P}\left(\{\mathbf{w}_k\}^{(r+1)}, \{\rho_k\}^{(r+1)}, \{\theta_m\}^{(r)}\right). \quad (37)$$

Similarly, in the step 8 of **Algorithm 1**, we can obtain IRS phase shift when $\{\mathbf{w}_k\}^{(r+1)}$ and $\{\rho_k\}^{(r+1)}$ are given. Accordingly,

$$\mathcal{P}\left(\{\mathbf{w}_k\}^{(r+1)}, \{\rho_k\}^{(r+1)}, \{\theta_m\}^{(r)}\right) \geq \mathcal{P}\left(\{\mathbf{w}_k\}^{(r+1)}, \{\rho_k\}^{(r+1)}, \{\theta_m\}^{(r+1)}\right). \quad (38)$$

Based on the above, we have

$$\mathcal{P}\left(\{\mathbf{w}_k\}^{(r)}, \{\rho_k\}^{(r)}, \{\theta_m\}^{(r)}\right) \geq \mathcal{P}\left(\{\mathbf{w}_k\}^{(r+1)}, \{\rho_k\}^{(r+1)}, \{\theta_m\}^{(r+1)}\right), \quad (39)$$

which shows that the value of the objective function is non-increasing after each iteration in the second stage of **Algorithm 1**. Since the objective function values of problems (P3.2), (P4.1) and (P5.1) have a finite lower bound, the convergence of **Algorithm 1** can be guaranteed.

IV. Numerical Results

In this section, we provide simulation results to demonstrate the effectiveness of the proposed JDBPR algorithm in IRS-assisted SWIPT NOMA networks. In this paper, we consider a three-dimensional (3D) coordinate system, where the BS and the IRS placed on the building are located at (0m, 0m, 15m) and (50m, 50m, 15m), respectively, and $K = 4$ ground users are randomly and uniformly distributed in a circle whose origin is (0m, 0m, 0m) and a radius of 200m. We consider that the BS is equipped with $N = 4$ antennas, and the IRS is equipped with 30 reflecting elements. We assume that the parameters of all users are the same, i.e., $\sigma_k^2 = \sigma^2$, $\delta_k^2 = \delta^2$, $\eta_k = \eta$, $\gamma_k = \gamma$ and $e_k = e$. Herein, we set $\sigma^2 = -70$dBm, $\delta^2 = -50$dBm and $\eta = 0.7$ in our numerical simulations. The path loss exponents are set as $\alpha_1 = 3$, $\alpha_2 = 2.2$ and $\alpha_3 = 2.5$. We set the path loss C_0 to -30dB when the reference distance is 1m, and we set the Rician factor to 3dB. The number of candidate random vectors used for the Gaussian randomization is set to 1000. The convergence threshold of the JDBPR algorithm is set as 10^{-3}. The simulation parameter table is shown in Table I.

We first evaluate the convergence performance of the proposed JDBPR algorithm. Fig. 3 shows the BS transmit power varies with the number of iterations under different IRS reflecting elements. It can be seen that as the number of iterations increases, the BS transmit power gradually decreases. The algorithm can reach convergence in the 8-th iteration, which verifies that the proposed algorithm converges fast. Specifically, we compare the performance of the JDBPR algorithm when the number of IRS reflecting elements are 30, 60, and 80 respectively. It can be seen that the greater the number of IRS reflecting elements, the lower the BS transmit power,

TABLE I
Simulation Parameters

Parameters	Value
Number of ground users	4
Number of antennas	4
Number of reflecting elements	30
The radius of circular area	200m
The coordinates of BS	(0m, 0m, 15m)
The coordinates of IRS	(50m, 50m, 15m)
The antenna noise power	-70dBm
The additional noise power	-50dBm
The path loss with reference distance of 1m	-30dB
The energy conversion efficiency	0.7
The path loss exponents	$\alpha = 3$, $\beta = 2.2$, $o = 2.5$
The Rician factor	-3dB
The number of candidate random vectors	1000
Convergence threshold	10^{-3}

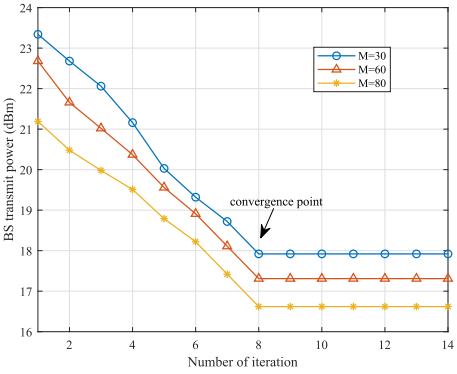

Fig. 3. The convergence of the proposed JDBPR algorithm.

which also verifies the effectiveness of the IRS assisted SWIPT NOMA networks.

Next, we compare the performance of the proposed JDBPR algorithm with other baseline algorithms. (1) EX-JBPR-opt algorithm: In the first stage, SIC decoding order adopts the exhaustive search method. The algorithm used in the second stage is the same as the second stage of the proposed JDBPR algorithm. (2) TS-JDBPR-opt algorithm: The proposed two-stage JDBPR algorithm. (3) TS-JDBPR-com algorithm: The algorithm is the same as the two stage optimization of the proposed JDBPR algorithm, except that the three sub-problems in the second stage of the former are not optimized alternately. (4) TS-JDBPR-ZF algorithm: The only difference from the TS-JDBPR-opt algorithm is that BS beamforming vector design uses the sub-optimal ZF beamforming scheme, which can eliminate user interference [15]. (5) TS-JDBP-ran algorithm: The only difference from the TS-JDBPR-opt algorithm is that the design of IRS phase shift adopts a random scheme.

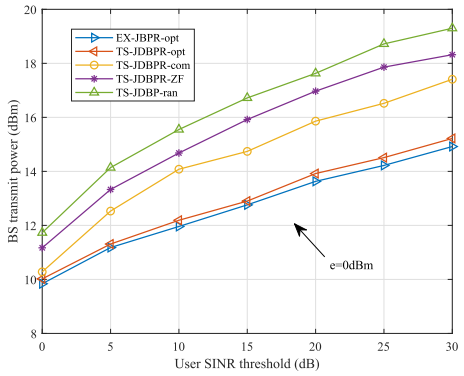

Fig. 4. The BS transmit power versus QoS thresholdwhen $e = 0$dBm.

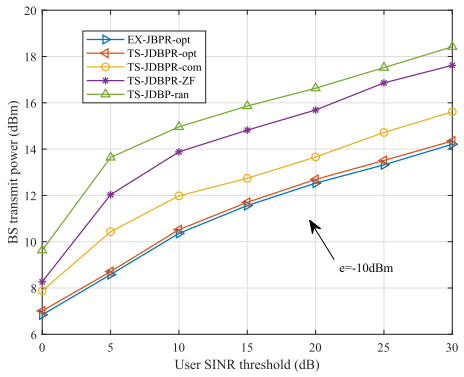

Fig. 5. The BS transmit power versus QoS thresholdwhen $e = -10$dBm.

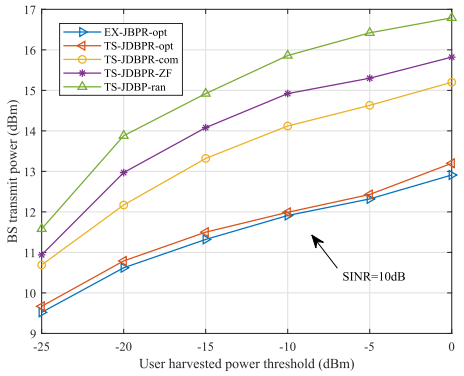

Fig. 6. The BS transmit power versus harvested powerwhen $\gamma_{th} = 10$dB.

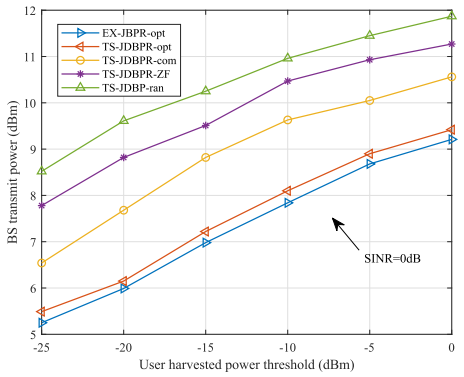

Fig. 7. The BS transmit power versus harvested powerwhen $\gamma_{th} = 0$dB.

Herein, we investigate the behavior of the BS transmit power with the QoS requirements of all users under different energy harvested threshold e. Fig. 4 and Fig. 5 respectively show how the BS transmit power varies with the users' QoS requirements under different energy harvested threshold (e.g. $e = 0$dBm and $e = -10$dBm). From Fig. 4 and Fig. 5, we can see that the BS transmit power under different algorithms increases with the increase of users' QoS threshold. This is because the larger the users' QoS threshold, the higher the requirements for the BS transmit power. In addition, it can be seen that the performance of the proposed TS-JDBPR-opt algorithm is similar to the EX-JBPR-opt algorithm, but the complexity of exhaustive search is much higher than the proposed algorithm. Meanwhile, our proposed TS-JDBPR-opt algorithm has better performance than the other three baseline algorithms. In specific analysis, the better performance of the TS-JDBPR-opt algorithm compared to the TS-JDBPR-com algorithm is mainly because the former is considered from the perspective of global optimization, while the latter only performs local optimization. Compared with the sub-optimal beamforming scheme of TS-JDPR-ZF algorithm, our proposed beamforming scheme at the BS has better performance. The TS-JDBP-ran algorithm designs the IRS phase shift in a random manner, thus the solution to our proposed algorithm has a better performance.

Fig. 6 and Fig. 7 elaborate how the BS transmit power varies with the user's energy harvested threshold under different users' QoS threshold (e.g. $\gamma = 10$dB and $\gamma = 0$dB). In general, as user energy harvested threshold increases, the BS transmit power continues to increase. This is mainly because the increase in the energy harvested threshold required by the user will require the BS to give a stronger transmission signal. When we consider that the users' QoS threshold is 10dB, it can be seen that the proposed TS-JDBPR-opt algorithm requires similar transmit power to the EX-JBPR-opt algorithm, but its complexity is much lower than the latter. This is mainly because the latter adopts the exhaustive search method in the decoding order scheme, which is more complicated. In addition, the performance of the TS-JDBPR-opt algorithm is also better than the other three baseline algorithms. The reason why the TS-JDBPR-opt algorithm performs better than the TS-JDBPR-com algorithm is that the latter does not achieve the convergence of the entire problem. Compared with the TS-JDBP-ran algorithm, the TS-JDBPR-opt algorithm can greatly reduce the BS transmit power, because that the TS-JDBP-ran algorithm does not optimize the IRS phase shift, and the random phase may even make the system performance worse. In addition, when the users' QoS threshold is 0dB, the change of the BS transmit power with the user's energy harvested threshold is similar to the former. Meanwhile, comparing Fig. 6 and Fig. 7, we can also see that when the user's energy harvested threshold is the same, the higher the users' QoS threshold, the greater the transmit power required by the BS.

Fig. 8 illustrates the variation of BS transmit power with the number of IRS reflecting elements under different algorithms. In general, it can be seen that as the number of IRS

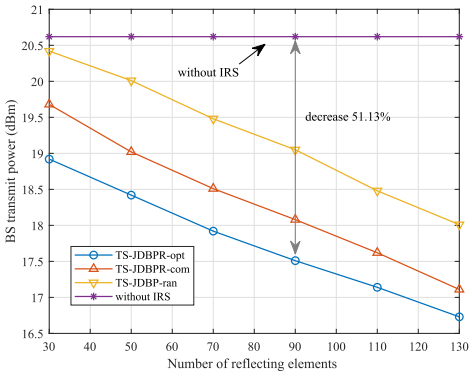

Fig. 8. The BS transmit power versus number of reflecting elements M.

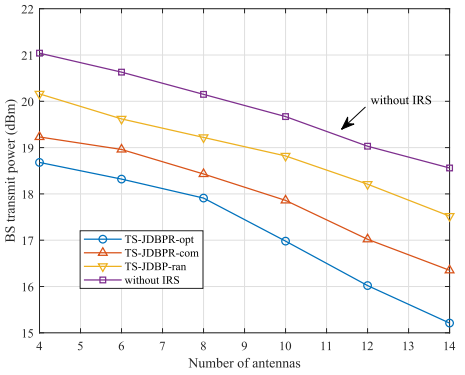

Fig. 9. The BS transmit power versus number of BS antennas N.

reflecting elements increases, the BS transmit power continues to decrease. This is because that the channel can be adjusted through the IRS, so that the system performance is enhanced, that is, the BS transmit power is gradually reduced. From Fig. 8, it can be seen that the performance of SWIPT NOMA networks with IRS assistance is better than the networks without IRS assistance. Furthermore, when the reflecting elements of IRS increase, the gap of this performance becomes larger, which also verifies that IRS has a very important auxiliary role in SWIPT NOMA networks. At the same time, our proposed TS-JDBPR-opt algorithm achieves a significant performance improvement compared to the TS-JDBPR-com algorithm and the TS-JDBP-ran algorithm. The main reason is that the TS-JDBPR-com algorithm does not achieve global convergence, and the TS-JDBP-ran algorithm does not optimize the IRS phase shift. Fig. 8 can also demonstrate that we can reduce the transmit power on the BS by increasing the number of IRS reflecting elements, and the cost of this scheme is very low.

Finally, Fig. 9 explains how the BS transmit power versus the number of BS antennas under different algorithms. With the increase of the number of antennas, the BS transmit power continues to decrease, which also shows that we can improve the performance of the system by increasing the number of BS antennas. This also motivates us to adopt massive MIMO systems to further enhance the IRS-assisted SWIPT NOMA networks. In addition, when the number of antennas is the same, the proposed TS-JDBPR-opt algorithm still yields a significant performance improvement compared to the TS-JDBPR-com algorithm and the TS-JDBP-ran algorithm.

V. Conclusion

This paper investigates the transmit power minimization problem for the IRS-assisted SWIPT NOMA networks. Specifically, under the users' QoS and energy harvested constraints, SIC decoding order, BS transmit beamforming vector, PS ratio, and IRS phase shift are jointly optimized. A two-stage optimization algorithm is proposed to solve this challenging problem. In the first stage, SIC decoding order determination algorithm based on the combined channel gain has been proposed. Further, we divide the second stage into three subproblems. The BS transmit beamforming vector, PS ratio and IRS phase shift are alternately optimized until convergence is achieved by applying SDR, SCA and Gaussian randomization. In addition, the computational complexity and convergence of the proposed JDBPR algorithm are analyzed and proved. Numerical results show that our proposed algorithm can significantly reduce the BS transmit power compared to other baseline algorithms, and the auxiliary role of IRS is extremely important, which can greatly relieve the pressure on the BS with low cost in practice.

Appendix A
Proof of Eq. (27)

Let $A_k = \sigma_k^2 + \frac{\delta_k^2}{\rho_k}$ and $A_{\bar{k}} = \sigma_{\bar{k}}^2 + \frac{\delta_{\bar{k}}^2}{\rho_{\bar{k}}}$. Take the logarithm of both sides of the constraint (26c) as follows

$$\ln\left(\frac{\mathbf{h}_k^H\mathbf{W}_k\mathbf{h}_k}{\sum\limits_{s(j)>s(k)}\mathbf{h}_k^H\mathbf{W}_j\mathbf{h}_k + A_k}\right) \leq \ln\left(\frac{\mathbf{h}_{\bar{k}}^H\mathbf{W}_k\mathbf{h}_{\bar{k}}}{\sum\limits_{s(j)>s(k)}\mathbf{h}_{\bar{k}}^H\mathbf{W}_j\mathbf{h}_{\bar{k}} + A_{\bar{k}}}\right), \text{ if } s(k) < s\left(\bar{k}\right), \quad (40)$$

which can also be expressed as

$$\begin{aligned}&\ln\left(\mathbf{h}_k^H\mathbf{W}_k\mathbf{h}_k\right) - \ln\left(\sum_{s(j)>s(k)}\mathbf{h}_k^H\mathbf{W}_j\mathbf{h}_k + A_k\right) - \ln\left(\mathbf{h}_{\bar{k}}^H\mathbf{W}_k\mathbf{h}_{\bar{k}}\right) \\ &\quad + \ln\left(\sum_{s(j)>s(k)}\mathbf{h}_{\bar{k}}^H\mathbf{W}_j\mathbf{h}_{\bar{k}} + A_{\bar{k}}\right) \\ &\leq 0, \text{ if } s(k) < s\left(\bar{k}\right). \end{aligned} \quad (41)$$

Since the first term and the fourth term on the left-hand-side (LHS) are both concave, we apply SCA to obtain their upper bound respectively, as follows,

$$\begin{aligned}\ln\left(\mathbf{h}_k^H\mathbf{W}_k\mathbf{h}_k\right) &\leq \ln\left(\mathbf{h}_k^H\mathbf{W}_k^{(r)}\mathbf{h}_k\right) \\ &\quad + \mathrm{Tr}\left(\left(\frac{1}{\mathbf{h}_k^H\mathbf{W}_k^{(r)}\mathbf{h}_k}\mathbf{h}_k\mathbf{h}_k^H\right)^H\left(\mathbf{W}_k - \mathbf{W}_k^{(r)}\right)\right) \\ &\triangleq \hat{f}_1\left(\mathbf{W}_k\right), \end{aligned} \quad (42)$$

and

$$\begin{aligned}\ln&\left(\sum_{s(j)>s(k)}\mathbf{h}_{\bar{k}}^{H}\mathbf{W}_{j}\mathbf{h}_{\bar{k}}+A_{\bar{k}}\right)\\ &\leq\ \ln\left(\sum_{s(j)>s(k)}\mathbf{h}_{\bar{k}}^{H}\mathbf{W}_{j}^{(r)}\mathbf{h}_{\bar{k}}+A_{\bar{k}}\right)+\sum_{s(j)>s(k)}\\ &\quad\times\mathrm{Tr}\left(\left(\frac{1}{\mathbf{h}_{\bar{k}}^{H}\mathbf{W}_{j}^{(r)}\mathbf{h}_{\bar{k}}}\mathbf{h}_{\bar{k}}\mathbf{h}_{\bar{k}}^{H}\right)^{H}\left(\mathbf{W}_{j}-\mathbf{W}_{j}^{(r)}\right)\right)\\ &\triangleq\ \hat{f}_{2}\left(\mathbf{W}_{j}\right).\end{aligned}\tag{43}$$

Therefore, constraint (26c) can be transformed into as follows Eq. (27). The proof is completed.

APPENDIX B
PROOF OF THE PROPOSITION 1

First, we introduce auxiliary variables and rewrite the problem (P3.2) as follows

$$\min_{\{\mathbf{W}_k\}}\ \sum_{k=1}^{K}\mathrm{Tr}\left(\mathbf{W}_{k}\right),\tag{44a}$$

$$\text{s.t. }\mathbf{h}_{\mathrm{k}}^{\mathrm{H}}\mathbf{W}_{\mathrm{k}}\mathbf{h}_{\mathrm{k}}-\gamma_{\mathrm{k}}\sum_{\mathrm{s(j)>s(k)}}\mathbf{h}_{\mathrm{k}}^{\mathrm{H}}\mathbf{W}_{\mathrm{j}}\mathbf{h}_{\mathrm{k}}\geq\gamma_{\mathrm{k}}\left(\sigma_{\mathrm{k}}^{2}+\frac{\delta_{\mathrm{k}}^{2}}{\rho_{\mathrm{k}}}\right),\tag{44b}$$

$$\hat{f}_{1}\left(\mathbf{W}_{k}\right)-\ln\left(\sum_{s(j)>s(k)}\mathbf{h}_{k}^{H}\mathbf{W}_{j}\mathbf{h}_{k}+A_{k}\right)-\ln\left(\mathbf{h}_{\bar{k}}^{H}\mathbf{W}_{k}\mathbf{h}_{\bar{k}}\right)+\hat{f}_{2}\left(\mathbf{W}_{j}\right)\leq 0,\text{if }s\left(k\right)<s\left(\bar{k}\right),\tag{44c}$$

$$\sum_{j=1}^{K}\mathbf{h}_{k}^{H}\mathbf{W}_{j}\mathbf{h}_{k}+\sigma_{k}^{2}\geq\frac{e_{k}}{\eta_{k}\left(1-\rho_{k}\right)},\tag{44d}$$

$$\varphi_{k}\leq\sum_{s(j)>s(k)}\mathbf{h}_{k}^{H}\mathbf{W}_{j}\mathbf{h}_{k}+A_{k},\tag{44e}$$

$$\phi_{\bar{k}}\leq\mathbf{h}_{\bar{k}}^{H}\mathbf{W}_{k}\mathbf{h}_{\bar{k}},\tag{44f}$$

$$\mathbf{W}_{k}\succeq 0.\tag{44g}$$

Since this problem is convex with respect to (w.r.t) $\mathbf{W}_k$, the Slater's condition holds [50]. Therefore, the duality gap is zero. By solving its dual problem, we can obtain its optimal solution. Let $\mathbf{H}_k=\mathbf{h}_k\mathbf{h}_k^H,\forall k$, the Lagrangian function corresponding to this problem can be given by

$$\begin{aligned}\mathcal{L}=&\sum_{k=1}^{K}\mathrm{Tr}\left(\mathbf{W}_{k}\right)-\sum_{k=1}^{K}\mathrm{Tr}\left(\mathbf{W}_{k}\mathbf{Y}_{k}\right)\\ &-\sum_{k=1}^{K}\lambda_{k}\mathrm{Tr}\left(\mathbf{W}_{k}\mathbf{H}_{k}\right)+\sum_{s\left(\bar{k}\right)>s(k)}\mu_{k\bar{k}}\\ &\times\mathrm{Tr}\left(\left(\frac{1}{\mathbf{h}_{k}^{H}\mathbf{W}_{k}^{(r)}\mathbf{h}_{k}}\mathbf{H}_{k}\right)^{H}\left(\mathbf{W}_{k}-\mathbf{W}_{k}^{(r)}\right)\right)\\ &-\sum_{\bar{k}=1}^{K-1}\upsilon_{\bar{k}}\mathrm{Tr}\left(\mathbf{W}_{k}\mathbf{H}_{\bar{k}}\right)-\sum_{k=1}^{K}\varpi_{k}\sum_{j=1}^{K}\mathrm{Tr}\left(\mathbf{W}_{j}\mathbf{H}_{k}\right)+\Upsilon,\end{aligned}\tag{45}$$

where Υ represents the sum of terms irrelevant to the proof. λ_k, $\mu_{k\bar{k}}$, $\upsilon_{\bar{k}}$ and ϖ_k are the Lagrangian multiplier, and $\mathbf{Y}_k\in\mathbb{C}^{N\times N}$ is the Lagrangian multiplier matrix. The dual problem of the problem is

$$\max_{\lambda_k,\mu_{k\bar{k}},\upsilon_{\bar{k}},\varpi_k>0,\mathbf{Y}_k\succeq 0}\ \min_{\mathbf{W}_k,\varphi_k,\phi_{\bar{k}}}\ \mathcal{L}.\tag{46}$$

Next, we use the Karush-Kuhn-Tucker (KKT) conditions to investigate the optimal solution structure of the dual problem. The KKT condition related to $\mathbf{W}_k^*$ can be given

$$\begin{aligned}K_1:\lambda_k^*,\mu_{k\bar{k}}^*,\upsilon_{\bar{k}}^*,\varpi_k>0,\mathbf{Y}_k^*\succeq 0,K_2:\mathbf{W}_k^*\mathbf{Y}_k^*=0,\\ K_3:\nabla_{\mathbf{W}_k^*}\mathcal{L}=0,\end{aligned}\tag{47}$$

where $\lambda_k^*,\mu_{k\bar{k}}^*,\upsilon_{\bar{k}}^*,\varpi_k$ and $\mathbf{Y}_k^*$ represent the optimal Lagrangian multiplers of the dual problem. $\nabla_{\mathbf{W}_k^*}\mathcal{L}$ denotes the gradient vector of Eq. (45) w.r.t $\mathbf{W}_k^*$. We can explicitly express K3 as follows

$$\mathbf{Y}_{k}^{*}=\mathbf{I}_{N}-\mathbf{\Delta},\tag{48}$$

where $\mathbf{\Delta}$ can be given by

$$\begin{aligned}\mathbf{\Delta}=\lambda_{k}^{*}\mathbf{H}_{k}-\sum_{s\left(\bar{k}\right)>s(k)}\mu_{k\bar{k}}^{*}\mathrm{Tr}\left(\frac{1}{\mathbf{h}_{k}^{H}\mathbf{W}_{k}^{(r)}\mathbf{h}_{k}}\mathbf{H}_{k}\right)\\ +\sum_{\bar{k}=1}^{K-1}\upsilon_{\bar{k}}^{*}\mathbf{H}_{\bar{k}}+\sum_{k=1}^{K}\varpi_{k}^{*}\mathbf{H}_{k}.\end{aligned}\tag{49}$$

Next, we will prove that the beamforming matrix $\mathbf{W}_k^*$ is rank-one by exploring the structure of $\mathbf{Y}_k^*$. We set the maximum eigenvalue of $\mathbf{\Delta}$ to $\zeta_{\max}$. It is worth noting that due to the randomness of the channel, the probability that multiple eigenvalues have the same maximum value is zero. According to Eq. (18), if $\zeta_{\max}>1$, $\mathbf{Y}_k^*$ cannot be positive semidefinite, which contradicts K_1. If $\zeta_{\max}<1$, $\mathbf{Y}_k^*$ must be positive definite and full rank. It can be seen from K_2 that $\mathbf{W}_k^*$ can only be $\mathbf{0}$, which is obviously contradictory to reality. Therefore, $\zeta_{\max}<1$ must hold, then $\mathrm{Rank}\left(\mathbf{Y}_k^*\right)=N-1$. Therefore, $\mathrm{Rank}\left(\mathbf{W}_k^*\right)=1$, i.e., the beamforming matrix $\mathbf{W}_k^*$ is rank-one. The proof is completed.

APPENDIX C
PROOF OF EQ. (30)

Let $B_{kk}=\left|\mathbf{h}_k^H\mathbf{w}_k\right|^2$, $B_{jk}=\sum_{s(j)>s(k)}\left|\mathbf{h}_k^H\mathbf{w}_j\right|^2+\sigma_k^2$, $B_{\bar{k}k}=\left|\mathbf{h}_{\bar{k}}^H\mathbf{w}_k\right|^2$ and $B_{j\bar{k}}=\sum_{s(j)>s(k)}\left|\mathbf{h}_{\bar{k}}^H\mathbf{w}_j\right|^2+\sigma_{\bar{k}}^2$. Then constraint (29c) can be rewritten as follows

$$\frac{B_{kk}}{B_{jk}+\frac{\delta_{k}^{2}}{\rho_{k}}}\leq\frac{B_{\bar{k}k}}{B_{j\bar{k}}+\frac{\delta_{\bar{k}}^{2}}{\rho_{\bar{k}}}},\ \text{if }s\left(k\right)<s\left(\bar{k}\right),\tag{50}$$

which can also be expressed as

$$\begin{aligned}B_{kk}B_{j\bar{k}}+B_{kk}\delta_{\bar{k}}^{2}\frac{1}{\rho_{\bar{k}}}-B_{\bar{k}k}B_{jk}-B_{\bar{k}k}\delta_{k}^{2}\frac{1}{\rho_{k}}\\ \leq 0,\ \text{if }s\left(k\right)<s\left(\bar{k}\right).\end{aligned}\tag{51}$$

Since the fourth term of LHS is concave, we can use SCA to obtain its upper bound, which can be given by

$$-\frac{1}{\rho_k} \leq -\frac{1}{\rho_k^{(r)}} + \frac{1}{\left(\rho_k^{(r)}\right)^2}\left(\rho_k - \rho_k^{(r)}\right). \tag{52}$$

Therefore, constraint (29c) can be transformed into as follows Eq. (30). The proof is completed.

APPENDIX D
PROOF OF EQ. (34)

Let $C_k = \sigma_k^2 + \frac{\delta_k^2}{\rho_k}$ and $C_{\bar{k}} = \sigma_{\bar{k}}^2 + \frac{\delta_{\bar{k}}^2}{\rho_{\bar{k}}}$. We take the logarithm of both sides of the constraint (33c), which can be expressed as

$$\ln\left(\frac{\mathrm{Tr}\left(\mathbf{S}_{k,k}\bar{\mathbf{U}}\right) + \left|\mathbf{q}_{k,k}\right|^2}{\sum\limits_{s(j)>s(k)}\left(\mathrm{Tr}\left(\mathbf{S}_{j,k}\bar{\mathbf{U}}\right) + \left|\mathbf{q}_{j,k}\right|^2\right) + C_k}\right) \leq \ln\left(\frac{\mathrm{Tr}\left(\mathbf{S}_{k,\bar{k}}\bar{\mathbf{U}}\right) + \left|\mathbf{q}_{k,\bar{k}}\right|^2}{\sum\limits_{s(j)>s(k)}\left(\mathrm{Tr}\left(\mathbf{S}_{j,\bar{k}}\bar{\mathbf{U}}\right) + \left|\mathbf{q}_{j,\bar{k}}\right|^2\right) + C_{\bar{k}}}\right). \tag{53}$$

Eq. (53) can also be given by

$$\begin{aligned}&\ln\left(\mathrm{Tr}\left(\mathbf{S}_{k,k}\bar{\mathbf{U}}\right) + \left|\mathbf{q}_{k,k}\right|^2\right)\\ &\quad - \ln\left(\sum_{s(j)>s(k)}\left(\mathrm{Tr}\left(\mathbf{S}_{j,k}\bar{\mathbf{U}}\right) + \left|\mathbf{q}_{j,k}\right|^2\right) + C_k\right)\\ &\quad - \ln\left(\mathrm{Tr}\left(\mathbf{S}_{k,\bar{k}}\bar{\mathbf{U}}\right) + \left|\mathbf{q}_{k,\bar{k}}\right|^2\right)\\ &\quad + \ln\left(\sum_{s(j)>s(k)}\left(\mathrm{Tr}\left(\mathbf{S}_{j,\bar{k}}\bar{\mathbf{U}}\right) + \left|\mathbf{q}_{j,\bar{k}}\right|^2\right) + C_{\bar{k}}\right) \leq 0.\end{aligned} \tag{54}$$

Since the first term and the fourth term on the LHS are both concave, we apply SCA to obtain their upper bound, which can be expressed as

$$\begin{aligned}\ln\left(\mathrm{Tr}\left(\mathbf{S}_{k,k}\bar{\mathbf{U}}\right) + \left|\mathbf{q}_{k,k}\right|^2\right) &\leq \ln\left(\mathrm{Tr}\left(\mathbf{S}_{k,k}\bar{\mathbf{U}}^{(r)}\right) + \left|\mathbf{q}_{k,k}\right|^2\right)\\ &\quad + \mathrm{Tr}\left(\left(\frac{1}{\mathrm{Tr}\left(\mathbf{S}_{k,k}\bar{\mathbf{U}}^{(r)}\right) + \left|\mathbf{q}_{k,k}\right|^2}\mathbf{S}_{k,k}^H\right)^H\left(\bar{\mathbf{U}} - \bar{\mathbf{U}}^{(r)}\right)\right)\\ &\triangleq \hat{g}_1\left(\bar{\mathbf{U}}\right),\end{aligned} \tag{55}$$

and

$$\begin{aligned}&\ln\left(\sum_{s(j)>s(k)}\left(\mathrm{Tr}\left(\mathbf{S}_{j,\bar{k}}\bar{\mathbf{U}}\right) + \left|\mathbf{q}_{j,\bar{k}}\right|^2\right) + C_{\bar{k}}\right)\\ &\quad \leq \ln\left(\sum_{s(j)>s(k)}\left(\mathrm{Tr}\left(\mathbf{S}_{j,\bar{k}}\bar{\mathbf{U}}^{(r)}\right) + \left|\mathbf{q}_{j,\bar{k}}\right|^2\right) + C_{\bar{k}}\right)\\ &\quad + \mathrm{Tr}\left(\left(\frac{1}{\left(\mathrm{Tr}\left(\mathbf{S}_{j,\bar{k}}\bar{\mathbf{U}}^{(r)}\right) + \left|\mathbf{q}_{j,\bar{k}}\right|^2\right) + C_{\bar{k}}}\right.\right.\\ &\quad \left.\left.\times \sum_{s(j)>s(k)}\mathbf{S}_{j,\bar{k}}^H\right)^H\left(\bar{\mathbf{U}} - \bar{\mathbf{U}}^{(r)}\right)\right) \triangleq \hat{g}_2\left(\bar{\mathbf{U}}\right).\end{aligned} \tag{56}$$

Therefore, constraint (33c) can be transformed into as follows Eq. (34). The proof is completed.

REFERENCES

[1] W. Qingqing and Z. Rui, "Towards smart and reconfigurable environment: Intelligent reflecting surface aided wireless network," *IEEE Commun. Mag.*, vol. 58, no. 1, pp. 106–112, Jan. 2019.

[2] W. Ni, X. Liu, Y. Liu, H. Tian, and Y. Chen, "Resource allocation for multi-cell IRS-aided NOMA networks," 2020, *arXiv:2006.11811*. [Online]. Available: http://arxiv.org/abs/2006.11811

[3] L. Lu, G. Y. Li, A. L. Swindlehurst, A. Ashikhmin, and R. Zhang, "An overview of massive MIMO: Benefits and challenges," *IEEE J. Sel. Topics Signal Process.*, vol. 8, no. 5, pp. 742–758, Oct. 2014.

[4] Q. Wu, W. Chen, M. Tao, J. Li, H. Tang, and J. Wu, "Resource allocation for joint transmitter and receiver energy efficiency maximization in downlink OFDMA systems," *IEEE Trans. Commun.*, vol. 63, no. 2, pp. 416–430, Feb. 2015.

[5] Y. Liu, Z. Qin, M. Elkashlan, Z. Ding, A. Nallanathan, and L. Hanzo, "Non-orthogonal multiple access for 5G and beyond," *Proc. IEEE*, vol. 105, no. 12, pp. 2347–2381, Dec. 2017.

[6] L. Dai, B. Wang, Y. Yuan, S. Han, C.-L. I, and Z. Wang, "Non-orthogonal multiple access for 5G: Solutions, challenges, opportunities, and future research trends," *IEEE Commun. Mag.*, vol. 53, no. 9, pp. 74–81, Sep. 2015.

[7] Y. Zhou, V. W. S. Wong, and R. Schober, "Coverage and rate analysis of millimeter wave NOMA networks with beam misalignment," *IEEE Trans. Wireless Commun.*, vol. 17, no. 12, pp. 8211–8227, Dec. 2018.

[8] F. Wei and W. Chen, "Low complexity iterative receiver design for sparse code multiple access," *IEEE Trans. Commun.*, vol. 65, no. 2, pp. 621–634, Feb. 2017.

[9] Y. Feng, S. Yan, Z. Yang, N. Yang, and J. Yuan, "Beamforming design and power allocation for secure transmission with NOMA," *IEEE Trans. Wireless Commun.*, vol. 18, no. 5, pp. 2639–2651, May 2019.

[10] Y. Cai, Z. Qin, F. Cui, G. Y. Li, and J. A. McCann, "Modulation and multiple access for 5G networks," *IEEE Commun. Surveys Tuts.*, vol. 20, no. 1, pp. 629–646, 1st Quart., 2018.

[11] Z. Ding *et al.*, "Application of non-orthogonal multiple access in LTE and 5G networks," *IEEE Commun. Mag.*, vol. 55, no. 2, pp. 185–191, Feb. 2017.

[12] Z. Ding *et al.*, "Impact of user pairing on 5G nonorthogonal multiple-access downlink transmissions," *IEEE Trans. Veh. Technol.*, vol. 65, no. 8, pp. 6010–6023, Aug. 2016.

[13] Y. Zeng, B. Clerckx, and R. Zhang, "Communications and signals design for wireless power transmission," *IEEE Trans. Commun.*, vol. 65, no. 5, pp. 2264–2290, May 2017.

[14] B. Clerckx, R. Zhang, R. Schober, D. W. K. Ng, D. I. Kim, and H. V. Poor, "Fundamentals of wireless information and power transfer: From RF energy harvester models to signal and system designs," *IEEE J. Sel. Areas Commun.*, vol. 37, no. 1, pp. 4–33, Jan. 2019.

[15] Q. Shi, L. Liu, W. Xu, and R. Zhang, "Joint transmit beamforming and receive power splitting for MISO SWIPT systems," *IEEE Trans. Wireless Commun.*, vol. 13, no. 6, pp. 3269–3280, Jun. 2014.

[16] X. Zhou, R. Zhang, and C. K. Ho, "Wireless information and power transfer: Architecture design and rate-energy tradeoff," *IEEE Trans. Commun.*, vol. 61, no. 11, pp. 4754–4767, Nov. 2013.

[17] Q. Wu and R. Zhang, "Intelligent reflecting surface enhanced wireless network via joint active and passive beamforming," *IEEE Trans. Wireless Commun.*, vol. 18, no. 11, pp. 5394–5409, Nov. 2019.

[18] Q. Q. Wu and R. Zhang, "Beamforming optimization for wireless network aided by intelligent reflecting surface with discrete phase shifts," *IEEE Trans. Commun.*, vol. 68, no. 3, pp. 1838–1851, May 2020.

[19] W. Tang *et al.*, "Wireless communications with programmable metasurface: New paradigms, opportunities, and challenges on transceiver design," *IEEE Wireless Commun.*, vol. 27, no. 2, pp. 180–187, Apr. 2020.

[20] C. Huang *et al.*, "Holographic MIMO surfaces for 6G wireless networks: Opportunities, challenges, and trends," *IEEE Wireless Commun.*, vol. 27, no. 5, pp. 118–125, Oct. 2020.
[21] X. Yuan, Y.-J. A. Zhang, Y. Shi, W. Yan, and H. Liu, "Reconfigurable-intelligent-surface empowered wireless communications: Challenges and opportunities," 2020, *arXiv:2001.00364*. [Online]. Available: http://arxiv.org/abs/2001.00364
[22] C. Liaskos, S. Nie, A. Tsioliaridou, A. Pitsillides, S. Ioannidis, and I. Akyildiz, "A new wireless communication paradigm through software-controlled metasurfaces," *IEEE Commun. Mag.*, vol. 56, no. 9, pp. 162–169, Sep. 2018.
[23] N. Rajatheva *et al.*, "White paper on broadband connectivity in 6G," 2020, *arXiv:2004.14247*. [Online]. Available: http://arxiv.org/abs/2004.14247
[24] S. Gong *et al.*, "Towards smart wireless communications via intelligent reflecting surfaces: A contemporary survey," 2019, *arXiv:1912.07794*. [Online]. Available: http://arxiv.org/abs/1912.07794
[25] J. Zhao, "A survey of intelligent reflecting surfaces (IRSs): Towards 6G wireless communication networks," 2019, *arXiv:1907.04789*. [Online]. Available: http://arxiv.org/abs/1907.04789
[26] W. Yan, X. Yuan, Z.-Q. He, and X. Kuai, "Passive beamforming and information transfer design for reconfigurable intelligent surfaces aided multiuser MIMO systems," *IEEE J. Sel. Areas Commun.*, vol. 38, no. 8, pp. 1793–1808, Aug. 2020.
[27] L. Dong and H.-M. Wang, "Enhancing secure MIMO transmission via intelligent reflecting surface," *IEEE Trans. Wireless Commun.*, vol. 19, no. 11, pp. 7543–7556, Nov. 2020.
[28] S. Hong, C. Pan, H. Ren, K. Wang, and A. Nallanathan, "Artificial-noise-aided secure MIMO wireless communications via intelligent reflecting surface," *IEEE Trans. Commun.*, vol. 68, no. 12, pp. 7851–7866, Dec. 2020.
[29] K. Zhi, C. Pan, H. Ren, and K. Wang, "Statistical CSI-based design for reconfigurable intelligent surface-aided massive MIMO systems with direct links," *IEEE Wireless Commun. Lett.*, vol. 10, no. 5, pp. 1128–1132, May 2021.
[30] T. Bai, C. Pan, Y. Deng, M. Elkashlan, A. Nallanathan, and L. Hanzo, "Latency minimization for intelligent reflecting surface aided mobile edge computing," *IEEE J. Sel. Areas Commun.*, vol. 38, no. 11, pp. 2666–2682, Nov. 2020.
[31] T. Shafique, H. Tabassum, and E. Hossain, "Optimization of wireless relaying with flexible UAV-borne reflecting surfaces," *IEEE Trans. Commun.*, vol. 69, no. 1, pp. 309–325, Jan. 2021.
[32] S. Li, B. Duo, X. Yuan, Y.-C. Liang, and M. Di Renzo, "Reconfigurable intelligent surface assisted UAV communication: Joint trajectory design and passive beamforming," *IEEE Wireless Commun. Lett.*, vol. 9, no. 5, pp. 716–720, Jan. 2020.
[33] H. Shen, W. Xu, S. Gong, Z. He, and C. Zhao, "Secrecy rate maximization for intelligent reflecting surface assisted multi-antenna communications," *IEEE Commun. Lett.*, vol. 23, no. 9, pp. 1488–1492, Sep. 2019.
[34] L. Lv, Q. Wu, Z. Li, N. Al-Dhahir, and J. Chen, "Secure two-way communications via intelligent reflecting surfaces," *IEEE Commun. Lett.*, vol. 25, no. 3, pp. 744–748, Mar. 2021.
[35] C. Wu, S. Yan, X. Zhou, R. Chen, and J. Sun, "Intelligent reflecting surface (IRS)-aided covert communication with Warden's statistical CSI," *IEEE Wireless Commun. Lett.*, vol. 10, no. 7, pp. 1449–1453, Jul. 2021.
[36] G. Zhou *et al.*, "A framework of robust transmission design for IRS-aided MISO communications with imperfect cascaded channels," *IEEE Trans. Signal Process.*, vol. 68, pp. 5092–5106, 2020.
[37] M. Fu, Y. Zhou, Y. Shi, and K. B. Letaief, "Reconfigurable intelligent surface empowered downlink non-orthogonal multiple access," 2019, *arXiv:1910.07361*. [Online]. Available: http://arxiv.org/abs/1910.07361
[38] B. Zheng, Q. Wu, and R. Zhang, "Intelligent reflecting surface-assisted multiple access with user pairing: NOMA or OMA?" *IEEE Commun. Lett.*, vol. 24, no. 4, pp. 753–757, Apr. 2020.
[39] J. Zuo, Y. Liu, Z. Qin, and N. Al-Dhahir, "Resource allocation in intelligent reflecting surface assisted NOMA systems," *IEEE Trans. Commun.*, vol. 68, no. 11, pp. 7170–7183, Nov. 2020.
[40] M. Zeng, X. Li, G. Li, W. Hao, and O. A. Dobre, "Sum rate maximization for IRS-assisted uplink NOMA," *IEEE Commun. Lett.*, vol. 25, no. 1, pp. 234–238, Jan. 2021.
[41] J. Zuo, Y. Liu, E. Basar, and O. A. Dobre, "Intelligent reflecting surface enhanced millimeter-wave NOMA systems," *IEEE Commun. Lett.*, vol. 24, no. 11, pp. 2632–2636, Nov. 2020.
[42] J. Zhu, Y. Huang, J. Wang, K. Navaie, and Z. Ding, "Power efficient IRS-assisted NOMA," *IEEE Trans. Commun.*, vol. 69, no. 2, pp. 900–913, Feb. 2021.
[43] Q. Wu and R. Zhang, "Weighted sum power maximization for intelligent reflecting surface aided SWIPT," *IEEE Wireless Commun. Lett.*, vol. 9, no. 5, pp. 586–590, May 2020.
[44] Q. Wu and R. Zhang, "Joint active and passive beamforming optimization for intelligent reflecting surface assisted SWIPT under QoS constraints," *IEEE J. Sel. Areas Commun.*, vol. 38, no. 8, pp. 1735–1748, Aug. 2020.
[45] C. Pan *et al.*, "Intelligent reflecting surface aided MIMO broadcasting for simultaneous wireless information and power transfer," *IEEE J. Sel. Areas Commun.*, vol. 38, no. 8, pp. 1719–1734, Aug. 2020.
[46] L. Subrt and P. Pechac, "Intelligent walls as autonomous parts of smart indoor environments," *IET Commun.*, vol. 6, no. 8, pp. 1004–1010, May 2012.
[47] J. Cui, Y. Liu, Z. Ding, P. Fan, and A. Nallanathan, "Optimal user scheduling and power allocation for millimeter wave NOMA systems," *IEEE Trans. Wireless Commun.*, vol. 17, no. 3, pp. 1502–1517, Mar. 2018.
[48] M. Grant and S. Boyd. (2014). *CVX: MATLAB Software for Disciplined Convex Programming, Version 2.1*. [Online]. Available: http://cvxr.com/cvx/
[49] A. Ben-Tal and A. Nemirovski, *Lectures on Modern Convex Optimization: Analysis, Algorithms, and Engineering Applications*. Philadelphia, PA, USA: SIAM, 2001.
[50] S. Boyd, S. P. Boyd, and L. Vandenberghe, *Convex Optimization*. Cambridge, U.K.: Cambridge Univ. Press, 2004.

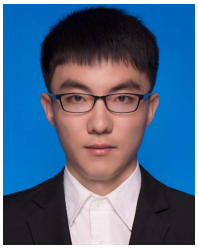

Zhendong Li received the B.S. degree in communications engineering from Zhengzhou University in 2017 and the master's degree in telecommunication and information systems from Beijing University of Posts and Telecommunications in 2020. He is currently pursuing the Ph.D. degree with the Broadband Access Network Laboratory, Department of Electronic Engineering, Shanghai Jiao Tong University (SJTU), Shanghai, China. His research interests include reconfigurable meta-surface (RMS), unmanned aerial vehicle (UAV) communications, space-air-ground (SAG) networks, the Internet-of-Things (IoT), and wireless resource management in future wireless networks.

Wen Chen (Senior Member, IEEE) is currently a tenured Professor with the Department of Electronic Engineering, Shanghai Jiao Tong University, China, where he is also the Director of the Broadband Access Network Laboratory. He has published more than 100 articles in IEEE journals and more than 120 papers in IEEE conferences, with citations more than 6000 in Google scholar. His research interests include reconfigurable meta-surface, multiple access, wireless AI, and green networks. He is a fellow of the Chinese Institute of Electronics and a Distinguished Lecturer of IEEE Communications Society and IEEE Vehicular Technology Society. He is Shanghai Chapter Chair of IEEE Vehicular Technology Society. He is an Editor of IEEE TRANSACTIONS ON WIRELESS COMMUNICATIONS, IEEE TRANSACTIONS ON COMMUNICATIONS, IEEE ACCESS, and IEEE OPEN JOURNAL OF VEHICULAR TECHNOLOGY.

Qingqing Wu (Member, IEEE) received the B.Eng. degree in electronic engineering from the South China University of Technology in 2012 and the Ph.D. degree in electronic engineering from Shanghai Jiao Tong University (SJTU) in 2016.

From 2016 to 2020, he was a Research Fellow with the Department of Electrical and Computer Engineering, National University of Singapore. He is currently an Assistant Professor with the State Key Laboratory of Internet of Things for Smart City, University of Macau. He has coauthored more than 100 IEEE papers with 20 ESI highly cited papers and 6 ESI hot papers, which have received more than 8000 Google citations. He was listed as a World's Top 2% Scientist by Stanford University in 2020. His current research interests include intelligent reflecting surface (IRS), unmanned aerial vehicle (UAV) communications, and MIMO transceiver design.

Dr. Wu was the exemplary reviewer of several IEEE journals. He was a recipient of the IEEE Communications Society Young Author Best Paper Award in 2021, the Outstanding Ph.D. Thesis Award of China Institute of Communications in 2017, the Outstanding Ph.D. Thesis Funding in SJTU in 2016, the IEEE ICCC Best Paper Award in 2021, and the IEEE WCSP Best Paper Award in 2015. He is the Workshop Co-Chair of IEEE ICC 2019-2022 Workshop on "Integrating UAVs into 5G and Beyond" and IEEE GLOBECOM 2020 and ICC 2021 Workshop on "Reconfigurable Intelligent Surfaces for Wireless Communication for Beyond 5G." He serves as a Workshops and Symposia Officer for Reconfigurable Intelligent Surfaces Emerging Technology Initiative and a Research Blog Officer for Aerial Communications Emerging Technology Initiative. He is the IEEE Communications Society Young Professional Chair in Asia–Pacific Region. He was the Exemplary Editor of IEEE COMMUNICATIONS LETTERS in 2019. He serves as an Associate Editor for IEEE COMMUNICATIONS LETTERS, IEEE WIRELESS COMMUNICATIONS LETTERS, IEEE Open Journal of the Communications Society, and IEEE OPEN JOURNAL OF VEHICULAR TECHNOLOGY. He is a Lead Guest Editor of IEEE JOURNAL ON SELECTED AREAS IN COMMUNICATIONS on "UAV Communications in 5G and Beyond Networks" and a Guest Editor of IEEE OPEN JOURNAL OF VEHICULAR TECHNOLOGY on "6G Intelligent Communications" and IEEE Open Journal of the Communications Society on "Reconfigurable Intelligent Surface-Based Communications for 6G Wireless Networks."

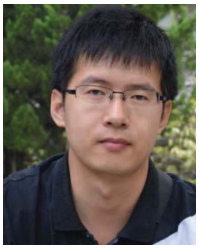

Kunlun Wang (Member, IEEE) received the Ph.D. degree in electronic engineering from Shanghai Jiao Tong University, Shanghai, China, in 2016. From 2016 to 2017, he was with Huawei Technologies Company Ltd., where he was involved in energy efficiency algorithm design. From 2017 to 2019, he was with the Key Laboratory of Wireless Sensor Network and Communication, SIMIT, Chinese Academy of Sciences, Shanghai. From 2019 to 2020, he was with the School of Information Science and Technology, ShanghaiTech University. Since 2021, he has been a Professor with the School of Communication and Electronic Engineering, East China Normal University. His current research interests include energy efficient communications, fog computing networks, resource allocation, and optimization algorithm.

Jun Li (Senior Member, IEEE) received the Ph.D. degree in electronic engineering from Shanghai Jiao Tong University, Shanghai, China, in 2009. From January 2009 to June 2009, he worked with Department of Research and Innovation, Alcatel Lucent Shanghai Bell, as a Research Scientist. From June 2009 to April 2012, he was a Post-Doctoral Fellow with the School of Electrical Engineering and Telecommunications, University of New South Wales, Australia. From April 2012 to June 2015, he was a Research Fellow with the School of Electrical Engineering, The University of Sydney, Australia. Since June 2015, he has been a Professor with the School of Electronic and Optical Engineering, Nanjing University of Science and Technology, Nanjing, China. He was a Visiting Professor at Princeton University from 2018 to 2019. His research interests include network information theory, game theory, distributed intelligence, multiple agent reinforcement learning, and their applications in ultra-dense wireless networks, mobile edge computing, network privacy and security, and the Industrial Internet of Things. He has coauthored more than 200 papers in IEEE journals and conferences, and holds one U.S. patents and more than ten Chinese patents in these areas. He served as a TPC member for several flagship IEEE conferences. He received an Exemplary Reviewer Award of IEEE TRANSACTIONS ON COMMUNICATIONS in 2018 and Best Paper Award from IEEE International Conference on 5G for Future Wireless Networks in 2017. He served as an Editor for IEEE COMMUNICATION LETTERS.